FINAL REPORT

RELATED STUDIES TO CATHODIC PROTECTION OF REINFORCED CONCRETE STRUCTURES

Report No. FHWA/OK 83(06)
Agreement No. 18
77-03-2

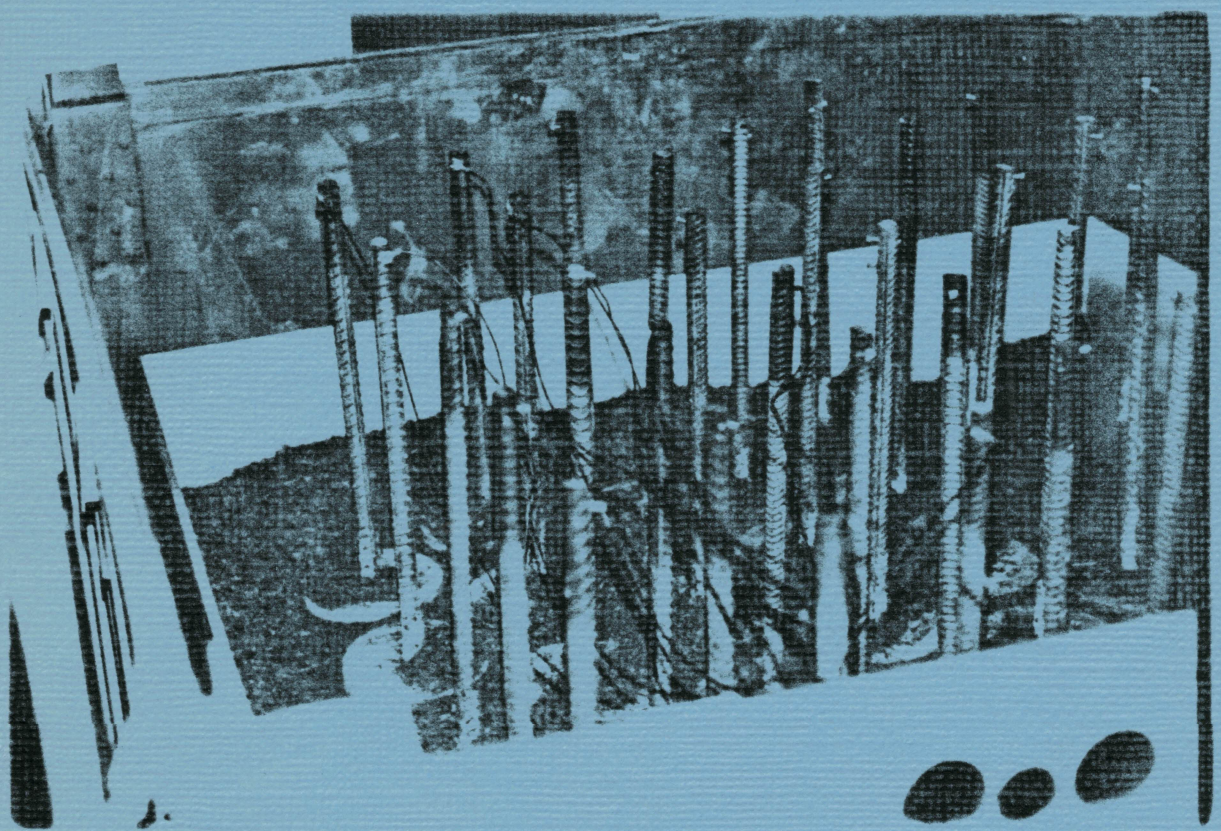

by

Carl E. Locke and Changiz Dehghanian

School of Chemical Engineering
and Materials Science

The University of Oklahoma

Norman, Oklahoma

TECHNICAL REPORT STANDARD TITLE PAGE

1. REPORT NO.	2. GOVERNMENT ACCESSION NO.	3. RECIPIENT'S CATALOG NO.
FHWA/OK 83(06)		

4. TITLE AND SUBTITLE	5. REPORT DATE
Related Studies to Cathodic Protection of Reinforced Structures	January, 1984
	6. PERFORMING ORGANIZATION CODE
7. AUTHOR(S)	8. PERFORMING ORGANIZATION REPORT
Carl E. Locke & Changiz Dehghanian	
9. PERFORMING ORGANIZATION NAME AND ADDRESS	10. WORK UNIT NO.
School of Chemical Engineering and Materials Science University of Oklahoma 202 West Boyd, Room 23 Norman, OK 73019	11. CONTRACT OR GRANT NO. Agreement 18 77-03-2
12. SPONSORING AGENCY NAME AND ADDRESS	13. TYPE OF REPORT AND PERIOD COVERED
Oklahoma Department of Transportation Research Division 200 NE 21st Street Oklahoma City, Oklahoma 73105	Final Report
	14. SPONSORING AGENCY CODE

15. SUPPLEMENTARY NOTES
Conducted in cooperation with the U.S. Department of Transportation, Federal Highway Administration

16. ABSTRACT Cathodic protection of steel in portland cement concrete requires information concerning several different areas. This report describes studies which were pointed toward developing an understanding of several of these.

A study of making an asphaltic concrete conductive was accomplished using coke breeze mixed with asphalt and aggregate. Mixes containing 45% coke breeze, 7-11% asphalt and the remainder a standard aggregate were found to be appropriate for conductive layers for cathodic protection.

It was found possible to determine corrosion rates electrochemically, using linear polarization. This laboratory technique gave corrosion rates similar to values obtained in other laboratories using other techniques.

Testing in the laboratory and bridge decks of molybdneum-molybdneum oxide electrodes indicated these would be useful as embeddable reference electrodes in concrete. Silver-silver chloride electrodes were not found to be stable in this application. These electrochemical half-cells, Mo/MoO_3, should prove to be useful for cathodic protection systems which require controlled potentials.

Reinforced concrete cylinders were exposed to cathodic protection level currents for five years. Pullout strengths and concentrations of sodium, potassium and chloride ions were determined throughout this time period. These data indicate the cathodic protection currents reduce the bond strength of the steel and concrete after about 3.5 years, due to accumulation of sodium and potassium at the interface between steel and concrete.

17. KEY WORDS	18. DISTRIBUTION STATEMENT
Cathodic Protection, Pull out strength Reference electrodes, Conductive asphaltic concrete	

19. SECURITY CLASSIF. (OF THIS REPORT)	20. SECURITY CLASSIF. (OF THIS PAGE)	21. NO. OF PAGES	22. PRICE
		103	

ACKNOWLEDGEMENTS

We would like to acknowledge the assistance of Dr. Joakim G. Laguros and his students on the conductive overlay studies.

We also acknowledge the assistance of Lane Gibbs and many other undergraduate students for conducting the experimental aspects of this project.

FINAL REPORT

Related Studies to Cathodic Protection of Reinforced Concrete Structures

Agreement No. 18

77-03-2

TO

Research Division

Oklahoma Department of Transportation

by

Carl E. Locke and Changiz Dehghanian

School of Chemical Engineering

and Materials Science

The University of Oklahoma

Norman, Oklahoma

Table of Contents

List of Tables

List of Illustrations

Executive Summary

Several different studies were carried out in this project concerning different aspects of cathodic protection of reinforcing steel in concrete. Experiments with conductive overlays, corrosion electrochemistry, reference electrodes, and effect of cathodic protection currents on pullout strength were conducted. Each of these are summarized below.

Coke breeze was blended with asphaltic concrete in order to make it electrically conductive. The electrically conductive asphaltic concrete overlays can be used to distribute cathodic protection currents on bridge decks. They must have a resistivity of 100 ohm-cm or less and a Hveen stability of 35 or greater. Mixes containing 45% coke breeze, 7-11% asphalt and the remainder a standard graded aggregate were found to meet these criteria. Therefore asphaltic concrete overlays can be used for a wearing course and current distribution layer.

Electrochemical experiments were conducted on steel embedded in concrete blocks. Linear polarization was used in conjunction with the standard anodic and cathodic polarization curves. The corrosion rates of steel in blocks containing levels of salt from 0 to 1% by weight of concrete were found to be 0.024 to 6.5 mpy.

An embeddable reference electrode is needed for cathodic protection installations on bridge decks. The molybdneum-molybdneum

electrode was tested during this study. This solid electrode was found to be stable with respect to time but some difficulty was found in reproducibility of electrode to electrode. However, these seem to offer some promise as reference electrodes for cathodic protection systems.

The effect of cathodic protection level currents, 3 ma/ft^2, on bond strength of rebars was tested over a five year period. The concentration of chloride, potassium and sodium ions as a function of time and cylinder diameter were determined as a part of this study.

The rebar pullout strengths of control and cathodically protected cylinder did differ significantly for the first three years. Differences were found after 42 months and at the end of the test the cathodically protected cylinders had a mean pullout strength about 21.3% lower than the control cylinders. There was substantial scatter in the data which leads to some concern on the certainty of the differences were significant. However, the conclusions reached in this study is that cathodic protection currents might cause a degradation of bond strength and this possibility should be studied in greater detail.

Introduction

The corrosion of reinforcing steel in portland cement concrete bridge decks (1,2) has become an increasing matter of concern. The rise in use of deicing salts has aggravated the problem since the chloride ion has been shown to be the primary cause of the corrosion of the steel. Various methods have been used to combat the deterioration of the decks. Epoxy coated rebars, galvanized rebars, overlays, membranes, inhibitors, polymer impregnation, and cathodic protection have been some of the methods used to slow or halt the deterioration. Each of these methods has advantages and limitation. This report is concerned with certain aspects of cathodic protection.

Cathodic protection is a tried and proven method for corrosion control. It has been used for close to 150 years to slow corrosion of metallic structures in the soil, fresh and sea water and in a variety of chemicals. However, it is only in the past 15-20 years that cathodic protection has been seriously considered for steel embedded in concrete (3,4,5).

Protection of the rebars in bridge decks presents some problems in the application of cathodic protection. It is difficult to distribute the current to the rebars. Measurement of the corrosion rate of the steel in the concrete is difficult. There is a need for a stable rugged reference electrochemical half cell that can be embedded in the concrete. There is a question concerning the potential damaging effects of the current flow through the portland cement concrete. These certainly are not all the problems

to be solved in the successful application of cathodic protection to bridge decks. However, they are the problems studied in this research project.

All these experiments are somewhat unrelated and were conducted as small sub projects. Each one is reported separately in the sections to follow.

Conductive Layer Study

Distribution of current across the surface of the bridge deck is a major problem of applying cathodic protection of steel in portland cement bridge decks. Portland cement concrete has a high electrical resistivity, 10^4 - 10^9 ohm-cm, depending on the moisture content. The lowest resistivity achieved, when it is fully saturated with water, is so high that lateral distribution of current is seriously impeded.

One approach to overcome this problem is to cover the surface of the bridge deck with a conductive layer. Contact with the conductive layer is made by means of a strip or plate anode. The layer, if conductive enough, then distributes the current laterally and acts as a sheet anode separated from the reinforcing steel only by the clear cover of the concrete.

The conductive overlay must support traffic directly or be covered in turn by a wearing course. In either method of usage, the layer must be stable in order to resist the vehicular weight.

This study was done to evaluate the possibilities of filling

an asphatic concrete with a conductive material like coke-breeze to produce a conductive layer with sufficient stability. An earlier project had evaluated the possibility of using filled polymeric membrane materials (6). This study indicated that it was possible to make the polymer materials conductive but the conductive materials like carbon black or coke-breeze stiffened the polymer to such an extent that it was too brittle to function as a membrane.

Electrochemistry and Corrosion Rate Study

Corrosion rates of steel in concrete have not been measured with any degree of accuracy. Several investigators have used "areas of rust" as a means to describe the relative corrosivity of steel in concrete with varying chloride concentration. However, it is difficult, if not impossible, to use the standard weight loss methods that have been used widely. An electrochemical technique, linear polarization has been studied in this project. As a part of this portion of the project the electrochemistry of steel in the concrete was also investigated.

Reference Electrodes

The potential range over which the steel can be cathodically protected when in concrete is relatively narrow ($\tilde{}$ 400 mv). In order to ensure that protection is effective and not destructive, the rebar potential should be controlled. The rebar potential is measured by comparing the rebars to another electrode with a

known stable potential. The most desirable comparison is done with a reference electrode which is an electrochemical half cell. Measurement of rebar potential on a bridge deck is a problem. Presently, the deck must be at least partially if not fully closed to traffic for the half cell survey as specified by ASTM C-876 using copper-copper sulfate ($Cu/CuSO_4$) reference electrodes. It would be a major advantage to be able to install reference electrodes in the bridge deck on a permanent basis. This would simplify the potential measurements and also would allow better control of the cathodic protection systems. An attempt to fabricate solid reference electrodes, molybdenum-molybdenum oxide (Mo/MoO_3) and silver/silver chloride (Ag/AgCl), was made in this study. The usefulness of these electrodes is reported.

Effect of Long Term Current Tests

Several experimental studies have been done on the effect of impressed current on the bond strength between the rebar and concrete. Most of these studies have been conducted at the current densities of 10^2 -10^3 ma/ft^2 over a relatively short period of time.

Casad (7) studied the effect of impressed currents (currents greater than 150 ma/ft^2) on the bond strength between the rebar and concrete for about a two month period. He found a drastic reduction in the bond strength for the test specimens (subjected to impressed current) in comparison to the control specimens (never received current).

Studies by the National Bureau of Standards (8) on the concrete cylinders subjected to a current equivalent to 400 ma/ft^2 (based on the rebar area) for a period of one year indicated the same results as found by Casad (7). They found 80% reduction in bond strength after one year of the test. They also observed that the concrete surrounding the rebar has been softened. Based on this investigation, they concluded that the migration of sodium and potasium ions were the main causes for the softening of the concrete.

Other investigators (9) studied the effect of different levels of current (in the ranges from 5 to 180 ma/ft^2) on the bond strength between the rebar and the concrete over a four year period. They found that the reduction in the bond strength was higher for higher levels of current. The reduction in bond strength also increased with time. However, the reduction in bond strength was small for the specimens subjected to 5 ma/ft^2. The migration of sodium and potassium ions occurs more slowly at the lower current densities. Therefore, longer time (more than 4 years) may be required to build up sufficient sodium and potassium ions at the regions near the rebar to cause a significant decrease in bond strength.

Hausmann (10) states that tests by the American Concrete Pressure Pipe Association indicate bond strength will not be significantly affected as long as the polarization potential is maintained less negative than -1.05 volts with respect to the saturated calomel electrode. This statement is related

primarily to the problem of hydrogen evolution which will occur at the cathode at about this potential (11).

However, if the bond failure is due to the ionic migration toward the rebar, damage could result at the lower currents if sufficient time was involved. This portion of the project will discuss the effect of low current (3 ma/ft^2, current in the range of cathodic protection applied to bridge decks) on the bond strength between rebar and concrete over a five year period. In addition, the effect of impressed current on the ionic migration of sodium, potassium and chloride ions over a five year period will be discussed.

Experimental Procedures

Conductive Layer Study

Asphaltic concrete mixes containing different amounts of coke-breeze and asphalt were prepared for both stability and resistivity tests. A standard asphalt cement obtained from ODOT was used in all mixes. A coke-breeze, like used in underground cathodic protection installations, was used to achieve the lowered resistivity. The types of coke-breeze used in the project varied in terms of gradation characteristics. Three gradations of coke breeze were used; one mix with a well distributed gradation curve (SCP), and two mixes with a very uniform, fine particle size gradation (Types A and B). Graphs of both gradation curves for the coke-breeze mixtures are shown in Figure 1. The (SCP)

coke-breeze mix had a uniformity coefficient of 10.4 while the finer, more uniform mix (Type B) had a uniformity coefficient of 1.83.

A matrix of mixes was developed so that an orderly approach to the optimum mix could be reached. Various mixes of asphaltic cement and coke-breeze was molded and then tested for stability and resistivity (Table 1). The molds were of the standard Hveem asphalt beam type (AASHTO Designation T190-731) and for each element of the mix matrix, three beams were molded: (1) a beam to test for resistivity, (2) a beam to test resistivity, the Hveem stability test and then another resistivity test, and (3) a control beam to be used if needed. The purpose of testing the second beam for resistivity after stability was to see if loading during stability testing affected the resistivity of the sample. The matrix of mix combinations, arrived at through discussion by the research team, are shown with the number of samples molded for each mix. For the particular matrix shown, the (SCP) coke-breeze was used.

The resistivity tests were obtained using the same procedure described previously for filled polymer materials (6).

Resistivity Measurements

A diagram of the circuit and apparatus used to measure the conductivity is shown in Figure 2. Copper strips were held against the ends of the sample with a clamp. A DC voltage was

applied to these strips to introduce current into the sample. The DC current was measured by using a voltmeter to determine the voltage drop across a decade resistance box in series with the current flow. The voltage drop through the sample was measured between two platinum tipped probes. The probes were mounted at a known distance apart in a polyethylene spacer which was placed on the top surface of the sample. The resistivity was then calculated as shown below:

$$\text{Resistivity} = \frac{V}{I} \frac{A}{D}$$

where V = voltage drop measured between probes

I = current flowing in circuit from power supply

A = cross sectional area presented to current flow

D = distance between probes

Electrochemistry and Corrosion Rate Study

Specimen Preparation

Three reinforcing bars ½ inch in diameter by 6 inches long were coated with an epoxy resin so that 6.9 $in.^2$ of the area was left bare. The applied coating was a mixture of 5 parts epoxy resin 828 and four parts of F-5 as the curing agent with 1.5 weight percent of Cab-o-Sil as thickener. The partially coated rebars were washed with acetone and symmetrically cast, 3 inches apart, in 6 x 12 inch concrete cylinders as shown in Figure 3. Several concrete cylinders were made, each containing sodium chloride ranging from 0 to 1 percent (based on concrete

weight). The concrete in each cylinder was mixed according to the Oklahoma Department of Transportation (ODOT) mix design as shown in Table 2.

Sodium chloride (NaCl) was dissolved in water and added to the mix. The specimens were then stored in the water cabinet for 28 days to cure.

After 28 days of curing the specimens were placed in laboratory dry condition for about a month and then the anodic and cathodic polarization curves combined with linear polarization were obtained to monitor the corrosion rate. The linear polarization tests were carried out galvanostatically on each specimen. The applied current increments were 0.05 to 2.4 μA, depending on the salt content. The anodic and cathodic polarization tests were carried out potentiostatically with ± 50 mv increments per three minutes. A $Cu/CuSO_4$ electrode served as the reference electrode. The $Cu/CuSO_4$ was placed against the concrete cylinder with potassium chloride wetted sponge as a contact point.

In the above tests a potentiostat model PEC-1B manufactured by Floyd Bell Associates, Inc., was used. In addition, the corrosion rates were monitored and compared with those obtained from a commercial corrosion rate measurement instrument (Petrolite model M-1013).

Reference Electrodes

The silver/silver chloride (Ag/AgCl) electrodes were prepared from reagent grade silver chloride and sixteen gauge fine silver wire, 1 mm in diameter. Two preparation methods were used; melt

casting and dipping. Molten silver chloride was poured around the wire in the melt casting method. The temperature of the molten silver chloride has an effect on the ultimate performance of the electrode. Best results were obtained with the melt temperature only slightly above the melting point. The electrodes were about 1.2 centimeters in diameter and 1.2 to 1.8 cm long.

Silver/silver chloride electrodes were also made by dipping silver wire into molten silver chloride. The wire was dipped several times into the silver chloride to build up the electrode like making candle by dipping. Dipping was done in different temperatures of silver chloride ranging from the melting point (230° C) to 540° C.

The molybdenum-molybdenum oxide (Mo/MoO_3) electrodes were made by oxidation of molybdenum metal in molten potassium nitrite at 380 to 400° C. Two procedures were used. The rods were made of an anode in an electrochemical cell while in the potassium nitrate in one method and were exposed only to the potassium nitrate in the other.

Both the Ag/AgCl and Mo/MoO_3 electrodes were soldered to insulate the copper wire. The joints were sealed with epoxy or silicone-seal compound.

Measuring Methods

The potential of these electrodes was compared to standard reference electrodes in NaCl solutions, saturated calcium hydroxide solutions containing various levels of NaCl and in portland cement

concrete. The concrete contained chloride ion concentration up to 0.5 percent by weight of the total concrete mix. At later dates, the Mo/MoO_3 electrodes were also tested in the laboratory dry and water saturated concretes containing Cl^- concentration higher than 0.5%. The reference electrodes used were saturated calomel electrode for measurements in aqueous solutions and $Cu/CuSO_4$ electrode for measurements in concrete.

Long Term Current Tests

Concrete Cylinders

The concrete for the test blocks was mixed and cast following the procedures prescribed in the ASTM C-234 for the rebar pull out strength test with one modification. The concrete test blocks were cast as cylinders 15 centimeters (6 inches) in diameter by 15 centimeters (6 inches) long. A number six steel rebar was embedded in the axis of each cylinder as shown in Figure 4.

The concrete in each cylinder was mixed according to the Oklahoma Department of Transportation mix design as shown in Table 2. Sodium chloride (NaCl) was added to each cylinder in an amount to give a concentration of about 0.1% based on weight of concrete. The specimens were stripped from their molds a day after casting and were cured for 28 days in 100% humidity atmosphere obtained by storing the cylinders in a closed cabinet in which water containers were placed.

One hundred and sixty cylinders were poured in eight batches. Eighty of these were under impressed cathodic currents. The remaining eighty were used as controls (never received current). Eighty cylinders under impressed current and eighty as controls were allowed four from each (test and control) to be tested each three months over a five year period.

At the end of the tests, it was discovered reinforcing steel with different deformation patterns had been used. Examination of the data, however, did not reveal any significant differences in the pullout strength due to the rebar type.

Current Apparatus

The current test cylinders were placed in wooden trays equally spaced apart. Coke-breeze was poured around the cylinders to provide a current path. High silicon iron button-shaped anodes were used to contact the coke-breeze. Forty cylinders were placed in each of two boxes and four anodes were placed in each corner of each box. Figure 5 is a diagram of the placement of anodes and cylinders. Figure 6 is a photograph of the cylinders in place in the trays. Each tray was enclosed in a tightly sealed box in which containers with water were placed to achieve a humid atmosphere.

The eighty control cylinders were placed in a box of the same size as the box containing the cylinders under impressed currents. Water containers were also placed in this box to provide humid atmosphere.

The current test apparatus was set up to deliver 3 ma/ft^2 current density to each rebar. Some difficulty was encountered in achieving an even distribution of current to each cylinder. The coke-breeze was repacked and the variable resistance connected

to each rebar was changed in order to accomplish this. The potential of steel was measured to be sure that it was below -1.0 volt with respect to $Cu/CuSO_4$. This was done to avoid hydrogen generation at the cathode which will certainly destroy the bond between rebar and concrete.

Figure 7 illustrates the circuitry used for control and measurement of the current to each cylinder. The cylinders were all wired in parallel. The current flow to each rebar was monitored by means of the voltage drop across a precision 100 ohm resistor in series with rebar. The current to each rebar was checked and readjusted periodically to a preset level by varying the series resistance. A 100 volt, 5 ampere constant voltage power supply was used to provide the necessary current.

Rebar Pull out Strength Test and Chemical Analysis

The cylinders were removed from the current apparatus at three month intervals for the five year period of the test. Four cylinders subjected to current flow and four as control with no current flow were removed from the test apparatus at each interval. The rebar pull out-strength test using ASTM C-234 was conducted on all eight cylinders. The force required to pull the reinforcing bar from the concrete cylinder was reported as the pull-out strength. In all cases this occured when the cylinder broke apart. After the pull-out test, the specimens were split open for visual inspection of the concrete and the rebar in the regions surrounding the rods.

The cylinders were poured in batches due to the capacity of the cement mixer available. The cylinders in each batch were evenly divided between control and current exposure test cabinets.

Equal number of cylinders from each batch were taken from the control and test cabinet at each test interval. This procedure was used in order to compare effect of current level on cylinders taken from the same mix batch.

In order to obtain the concentration profiles for sodium, potassium and chloride ions as a function of distance from rebar, the samples of concrete were obtained at three sections of each concrete cylinders: adjacent to rebar; 3.75 cm (1.5 inches) far from rebar; and at the concrete surface. The samples were obtained by hammer drilling into the concrete without use of water. The samples from the concrete surface were taken by drilling into the sections on the concrete surface. The samples from the region near the rebar were taken by drilling through the concrete pieces separated from the section adjacent to the rebar and finally the samples from the midsection were obtained by drilling first through the concrete surface to reach the midsection and the samples were collected from there.

Ten to fifteen concrete samples were obtained at each location for each cylinder. These powdered samples were obtained at each location for each cylinder and were combined for the analyses. Each combined sample was divided into ten portions for the cation determinations and five portions were taken of each for the chloride analyses. The chemical analyses for determining potassium and sodium ions in concrete were made by dissolving the concrete powder with acid and then the solution was analyzed using atomic absorption as described by Perkin Elmer (12).

The chloride content of concrete at the regions mentioned above was determined using the modified Berman method (13).

RESULTS

Conductive Layer Study

Gradation curves are shown comparing the aggregate without coke-breeze and the aggregate mix with 15% coke-breeze added, compared to the limits of the Type C mix in the specifications (Figure 8). It is to be noted that with 15% coke-breeze added, the mix still falls within specification limits. Also, a typical data sheet, showing aggregate and coke-breeze calculations, illustrates how various percentages were arrived at in calculating mixes (Table 3). The coke-breeze replaced aggregate and the amounts of rock, screenings and sand normally added to achieve a Type C mix were changed. In this particular data sheet, 25% coke-breeze was used.

To present the stability and resistivity data, plots were made on the same graph for constant percentages of asphalt but varying the percentage of coke-breeze. The Type C specifications establish a minimum Hveem Stability Number of 35, and this limit is also shown on each graph (Figures 9, 10, 11, and 12). It should be noted that 5% asphalt was not enough for the 25, 35, 45 and 55% coke-breeze mixtures while 13% asphalt proved too high for the 15, 25, 35% coke-breeze mixtures. It is not possible to collect very much data for these mixes.

Extraction tests were performed on two control beams of the 25% coke-breeze mix. Gradation curves were plotted

for the aggregate, including the 25% coke-breeze, before mixing and then after stability tests and extraction. This was done to compare the two curves and establish if any coke-breeze breakdown was occuring during loading in the stability test. One of these plots is shown and it indicates very little, if any, breakdown (Figure 13). The slight difference is probably attributable to the extraction test variability.

Further Test Results

Using some of the results of the (SCP) coke-breeze mixtures, certain combinations of mixes were eliminated as unworkable and smaller mix matrices were set up to analyze the finer coke-breeze products. Two, very similar, fine coke-breeze mixes were used. They were labeled types A and B, and the gradation for type B is shown in Figure 1.

After mixing various samples, it was observed that both types (A and B) were unworkable. They formed very viscous type beams with virtually no stability. An extraction test was performed on one sample with 25% coke-breeze added, and the gradation plotted against the 25% (SCP) coke-breeze mix. The differences are very notable and vary as much as 20% passing in the area of the No. 40 sieve (Figure 13).

Using resistivity data, it was also determined that stability did not alter the resistivity data on the samples mixed with the (SCP) coke-breeze or the samples molded with the fine coke-breeze types (A and B).

Electrochemistry and Corrosion Rate Study

Both anodic and cathodic polarization curves for steel in concrete containing 0 to 1 percent NaCl are shown in Figure 14. The results show that the anodic and cathodic current densities increased with an increase in salt concentration. The increase in the current densities are indicative of more severe corrosion. The increases in the current density were more dramatic for salt concentrations above 0.1%. These polarization curves were also used to obtain the Tafel slopes for use in the linear polarization as a corrosion rate measuring method. Typical linear polarization curves obtained in this study are shown in Figure 15. Not all the data were as linear as shown in this figure. Some had more curvature. However an attempt was made to obtain the average slopes from these curves. These slopes and the Tafel slopes determined from the polarization curves were used to calculate the corrosion rates.

Table 4 contains the calculated corrosion rates based on these data. In addition, the corrosion rates determined by the PAIR meter manufactured by Petrolite Corporation are also given in this table. As can be seen, the corrosion rate increased with increase in the salt concentration. The corrosion rates determined by the Commercial instrument (PAIR meter) using three electrode probes are much lower than those obtained from the linear polarization method.

However, the relative increase in corrosion rates with salt concentration was the same as those shown by linear polarization method.

Reference Electrodes

Silver/Silver Chloride (Ag/AgCl) The data presented here are for a batch of 11 molded Ag/AgCl electrodes tested in solutions. It was necessary to reject four of these electrodes, due to large potential deviations from the average.

Table 5 contains the average potential measured over a total of 108 days. The data taken in salt solutions pertain to the first 30 days after preparation. The measurements in the $Ca(OH)_2$ solutions were taken for the period of 30 to 68 days after they were made. The electrodes were then stored in saturated $Ca(OH)_2$ and measured in the $Ca(OH)_2$ containing chloride ion. These data can be compared to the values given in Table 6, which were calculated from the electrode potential of Ag/AgCl in 0.1 N KCl given as 0.2888 v in the literature (14). The Nernst equation was used to correct the potential for chloride ion activity. The potential values were affected by hydroxyl ion which is not predicted from the Nernst equation.

These same electrodes were then cast in 6 x 12 inch concrete cylinders. Each concrete cylinder had one steel rebar about ½ inch in diameter and 10 inches long. The chloride content in the cylinders was 0.1, 0.2 and 0.5%.

The values obtained at 40 days after the electrodes were placed into the concrete are tabulated in Table 7. However, the potentials of these electrodes did not remain stable and steady after 70 days in concrete.

Molybdenum/Molybdenum Oxide, Mo/MoO_3 The oxide formed on the molybdenum electrodes was removed with a file and analyzed by x-ray diffraction. These data indicated that the temperature of the molten potassium nitrate affected the type of oxide formed on the molydenum. When the temperature was between the melting point (333°C and 400°C), the oxide formed was the trioxide, MoO_3. When the temperature of KNO_3 was raised above 400°C, the KNO_3 decomposed and the oxide formed was the dioxide (MoO_2). The potential and stability of these electrodes are dependent upon the oxide formed.

The potentials of the electrodes were measured while immersed in sodium hydroxide (NaOH) solutions ranging in concentration up to 40 percent by weight. Figure 16 illustrates this variation of potential with respect to NaOH concentration. These data agree with those reported by Every and Banks (15).

The potentials of the electrodes as a function of time are shown in Figure 17. These data were obtained with the electrodes immersed in saturated $Ca(OH)_2$ compared to a saturated calomel cell. Figure 18 contains similar data for those electrodes as a function of salt concentration. The agreement between electrodes is good. These electrodes

were placed in concrete cylinders containing various concentrations of chloride ion content. Figure 19 illustrates the potential of the Mo/MoO_3 electrodes compared to a $Cu/CuSO_4$ as a function of chloride ion content. In addition, the potential of the steel rebar compared to the $Cu/CuSO_4$ is given. Figure 20 illustrates the rebar potential compared to $Cu/CuSO_4$ and to Mo/MoO_3. These data were taken during the 28 days the cylinders were curing in the water cabinet.

Figure 21 is a plot of the electrode potentials compared to $Cu/CuSO_4$ as a function of time. The electrode potential begins to shift at about the same time the cure period is over. These electrodes had been made by both methods listed, with and without electrolysis. There was no discernible difference between the ones made with electrolysis and those made without.

The potential of the electrodes shown in Figure 20 was monitored after 8 months for batch 1 and 6 months for batch 2. In addition, a third lot of electrodes had been in cylinders for four months. Table 8 contains the average potential of all these electrodes (21 total). The effect of chloride ion on the potential of the electrodes in concrete containing 0 and 0.5% chloride are within the standard deviations while the potential of the electrodes in concrete with 0.1 and 0.2 on chloride shifted by about 30-40 mv.

The potential of Mo/MoO_2 electrodes were not steady with respect to time.

Other batches of Mo/MoO_3 electrodes were manufactured later. The potential of these electrodes was measured after they were immersed in saturated calcium hydroxide, then they were embedded in concrete with chloride concentration varying from 0 to 2.1%. These concrete samples were soaked in distilled water and the potential of the electrodes was measured with time. Table 9 gives the potentials of the electrodes in water-saturated concrete as a function of chloride concentration. It is interesting to note that the electrode potentials were in the range of -550 to -600 mv vs $Cu/CuSO_4$ for the concrete containing low chloride concentration up to 0.6%. However, the potentials of these electrodes were more negative at the higher chloride concentration, but they remained constant with time.

The potentials of some of the Mo/MoO_3 electrodes which had been in the laboratory dry concrete for five years were measured with an external $Cu/CuSO_4$ electrode. The potential of these electrodes as a function of distance from the $Cu/CuSO_4$ was also determined. Then the same concrete sample was soaked in distilled water for two weeks and the potential of these electrodes as a function of distance from $Cu/CuSO_4$ was measured again as shown in Tables 10 and 11. The results indicated that an increase in the distance between Mo/MoO_3 embedded in dry concrete and an external $Cu/CuSO_4$ makes a dramatic difference in potential. The potential of these electrodes became more positive when the distance between

$Cu/CuSO_4$ and Mo/MoO_3 increased. However, the potential of the electrodes in the same concrete sample when soaked in distilled water for two weeks shifted toward a more negative value (-550 to -600 mv vs $Cu/CuSO_4$) and an increase in the distance between $Cu/CuSO_4$ and the Mo/MoO_3 electrodes had no effect on their potentials.

In addition, some Mo/MoO_3 electrodes were also used in a bridge deck on State Highway 51 about 5.6 miles east of the Payne County line. The potential of these electrodes was monitored monthly. The potential of the electrodes was in the range of -174 to -370 mv vs an external $Cu/CuSO_4$ electrode nine to ten months after the installation. The distance between $Cu/CuSO_4$ and Mo/MoO_3 electrodes affected the potential as found to be the case in the laboratory experiments. However, the potentials were fairly stable with time when the $Cu/CuSO_4$ was placed in the same position as the previous measurements.

Effect of Long Term Current Tests

The data on pull-out strength are presented in tabular form and as plots of pull-out strength as a function of time. Tables 13-17 contain the pull-out strength data for each cylinder grouped in the test year. The batch number for each set is also identified. The average of all cylinders sampled in one year, standard deviation, standard error of the mean, and fractional standard deviation of each year's samples are listed for the control cylinders and the cylinders under cathodic protection.

Table 18 lists the mean pull-out strength for each set of cylinders listed by batch number. Table 19 lists the same data organized by set number.

The yearly average data are shown in Table 20 and Figure 22. The data presented in this manner are substantially smoothed

and indicate there are differences in the pull-out strengths that may be significant. As an example in Table 17, the standard error of the mean for the cylinders exposed to cathodic protection currents is 789 psia. There is a 68.3% certainty the true value is 15,647 (the mean value) ± 789 psia and a 95.5% certainty the true value is 15,647 ± 1578 psia. Since the mean for the control sample is 19,873 psi with a standard error of the mean of 810 psi, there is a high degree of certainty (better than 94.5%) the means are significantly different.

When the values of pull-out strength for all cylinders were used in a quadratic regression statistical package, the plotted differences look to be similar to the values plotted from the yearly averages. Figure 22A is the computer generated plot of this analysis. This plot also indicate the scatter obtained in each data set.

The concentration of potassium ions (K^+) at the region near the rebar surface was determined as a function of time for the test and control specimen is shown in Figure 23. Each point on the curves is the average of the forty sample analyses taken from four identical cylinders. The results show that the concentration of K^+ near rebar increases as the exposure time to the impressed current increases. There was some scattering in the data from one batch of cylinders to another which may be due to sampling. A comparison between the specimen subjected to impressed current and the control cylinders also indicates higher K^+ accumulation near the rebar for test cylinders than that for control ones. This figure also shows that the K^+ concentration near the rebar for the test and control (never received current) specimen was approximately the same or close for a period of up to 18 months. However, the K^+ accumulation near the rebar for the test specimen became

much higher than that for the control cylinders after 18 months of exposure. These differences in the K^+ concentration became greater with time. For instance, the K^+ concentrations determined for test and control specimen after 39 months of exposure were 0.18% and 0.10%, respectively, in comparison to the concentration determined at 57 months which was about 0.25% and 0.13% for test and control specimen, respectively.

Figure 24 gives the results of K^+ concentration determined at the concrete surface (3 inches away from the rebar) for the test and control specimen. The results indicate that the K^+ concentration at the concrete surface is higher for the control specimen than that for the test cylinders. These differences became more drastic with time. The comparison of this figure with Figure 23 shows that K^+ ions migrate from the concrete surface toward the regions near the rebar for the specimen subjected to the impressed current. In the control specimen the K^+ ions migrate from the vicinity of the rebar toward the concrete surface.

Figure 25 gives a typical K^+ concentration profile as a function of distance from the rebar for the test and control specimen after 4.5 years of exposure time. The results show that for the test specimen the concentrations of K^+ from the concrete surface (shown as F) and at the regions of 3.75 cm (1.5 inches) away from the rebar (shown as M) are less than the K^+ concentration at the regions near the rebar (shown as N).

This is indicative of the K^+ migration toward the regions near the rebar. However, in the control specimen, the concentration of K^+ at the regions near the rebar (N) and at the regions of 3.75 cm (1.5 inches) away from the rebar (M) is less than that at the concrete surface. This indicates that the K^+ ions migrate from the regions near the rebar toward the concrete surface for the control specimen.

The results presented in Figures 26 and 27 are the sodium ion (Na^+) concentration as a function of exposure time to the impressed current. There was some scattering in the data from one batch of concrete cylinders to another which is probably due to sampling. Each point on these curves represents the average of 40 sample analyses taken from four identical test cylinders. Figure 26 shows that the Na^+ concentration at the regions near the rebar for the specimen subjected to the impressed current increases as the exposure time increases. The Na^+ concentration at the regions near the rebar for the specimen subjected to the impressed current increases as the exposure time increases. The Na^+ concentrations near the rebar for the test specimen are higher than that for the control cylinders. Figure 27 shows that the concentrations of Na^+ at the concrete surface for the test specimen are less than that for the control specimen. From the comparison between Figures 26 and 27 it appears that Na^+ ions migrate from the concrete surface toward the regions near the rebar.

However, the direction of the migration is opposite for the control specimens.

A typical concentration profile for Na^+ ions as a function of distance is shown in Figure 28. Again the results show that Na^+ ion accumulation at the regions near the rebar is higher than that in middle section (1.5 inches away from the rebar) and ions at the concrete surface for the specimen subjected to the impressed current. Therefore, it seems that in the test specimen the Na^+ ions like the K^+ ions migrate toward the rebar section. However, for the control specimen the general trend is opposite and Na^+ concentration at the concrete surface (shown as F) is higher than the M section (1.5 inches far from the rebar) and the region near the rebar (shown as N).

Plots shown in Figures 29 and 30 are the results of the chloride analysis taken from the region near the rebar and the region at the concrete surface, respectively. Each point on the curves is the average of 20 sample analyses from the four identical cylinders. The results indicate that in contrast to K^+ and Na^+ ions the Cl^- ion concentrations at the region near the rebar for the treated specimen are lower than those in the control specimen. The Cl^- concentration at the concrete surface for the test specimen is higher than that in the control specimen. This suggests that Cl^- ions in the test specimen migrate toward the concrete surface with time. However, in the control specimens, the Cl^- concentration at

the concrete surface was lower than that at the mid-section and the region near the rebar. The concentration on the concrete surface was even lower than that at the mid-section and the region near the rebar. The concentration on the concrete surface was even lower than 0.06% Cl^-. This is surprising because the amount of Cl^- added to these cylinders during casting was about 0.06%. In addition, the aggregate and cement in concrete contain a small amount of Cl^-.

Figure 31 gives a typical Cl^- concentration profile as a function of distance from the rebar after 4.5 years of exposure time. The results show that in the test specimens the Cl^- concentration at the region near the rebar and the M section (1.5 inches away from the rebar) is lower than at the concrete surface. However, in the control specimen the Cl^- concentration at the region near the rebar and the M section (1.5 inches far from the rebar) was approximately the same as the sum of 0.06% Cl^- which was initially added to each cylinder and the small amount of Cl^- which was originally contained in the aggregate used for concrete. The Cl^- concentration at the concrete surface was lower than that in the region near the rebar.

DISCUSSION

Conductive Layer Study

The conductive layer should have a resistivity of less than 100 ohm-cm for best results in the cathodic protection

system. In addition, it should have a Hveem stability above 35. The data indicate mixes containing 7-11% asphalt with 45% coke breeze meet these criteria. Table 12 lists the acceptable mixes with their respective resistivity and stability values.

However, these test results should be confirmed by field trials. There may be problems of mixing and application on site. The mixes proposed here are similar to those proposed by other investigators (4).

Electrochemistry and Corrosion Rate Study

The corrosion rates obtained in this study are surprisingly low when viewed in the light of the amount of damage due to corrosion in a bridge deck. However, the corrosion product is less dense than steel, the concrete has a low tensile strength, and traffic action is an aggravating factor. Generally, the corrosion rates for 0, 0.05, 0.08, 0.1 percent salt are almost identical. This indicates that the percentages of Cl^- mixed in concrete are not sufficient to cause any serious problem considering that some of the Cl^- may react with the concrete matrix as reported by Metha (17) and Ben Yair (18).

Gouda etal. (19) found the corrosion rate in slag cement concrete to vary from 0.05 to 0.34 mpy with $CaCl_2$ contents of 0 to 5 weight percent. These data were obtained using the same procedure as in this study. Alekseev and Rozental (20) found corrosion rates of 0.1 to 0.8 MPY for steel in concrete

after 3 years storage in a 90 percent relative humidity atmosphere. These data were obtained apparently by weight loss measurements.

Griffin and Henry (21) used the resistance type probes and found corrosion rates of 0 to 12 MPY in concrete containing up to 2.4 percent NaCl. They indicate one corrosion rate of 40 MPY at 0.6% NaCl. This seems somewhat questionable.

The results obtained in this study showed an increase in corrosion rate of about one order of magnitude between NaCl concentrations of 0.1 to 0.2 weight percent. This is in good agreement with the chloride concentration threshold theories (22) and the suggested value of 2 lb/yd^3 of Cl^- ion as the critical concentration in bridge decks (23).

In addition, the corrosion rates determined by commercial instrument were much lower than those determined by the linear polarization method but the relative corrosion rate trend as a function of Cl^- contents was the same. This may suggest that the use of commercial instrument in concrete due to the high resistivity of concrete may not be suitable if the IR drop is not compensated.

Reference Electrodes

The potential of the Ag/AgCl electrodes that were made in this study did not agree exactly with the potentials calculated with the Nernst equation. This was not surprising in light of the statement made by Ives and Janz (24) concerning reproducibility of the solid state. In addition, the manufacturing

methods used in this study led to many other problems. The electrolytic methods used by many other investigators may have provided electrodes with better electrochemical characteristics. However, the silver/silver chloride layer on these is fragile and susceptible to physical damage.

The potentials of the electrodes are affected by the chloride ion. The variation in potential was found to be of the order of 20-30 mv for the first two months of casting in concrete. However, the potentials of these electrodes were unstable and irreproducible after three months in concrete. This may be due to the loss of electrical contact between the electrodes and concrete as the water content of the concrete evaporates. Therefore, this prevents the use of this electrode in dry concrete like a bridge deck.

The molybdenum-molybdenum oxide (Mo/MoO_3) electrodes are a stable reference when manufactured to produce MoO_3 on the surface. The behavior of the electrodes with varying OH^- concentration is predicted by the half cell reactions (24).

$$Mo^{+6} + 6e^- \rightleftarrows Mo$$

$$MoO_3 \rightleftarrows Mo^{+6} + 3O^=$$

$$3O^= + 3H_2O \rightleftarrows 6OH$$

$$6OH^- + 6H^+ \rightarrow 6H_2O$$

The electrode should not be affected by the chloride ion as a theoretical basis. It was not possible to compare potentials from the literature since little work has been done with this electrode. Banks and Every (15) proposed

the manufacturing methods used in this study. However, they published little data on the electrode.

The potentials of these electrodes in concrete placed in laboratory-dry condition shifted toward a more positive direction for the first two months after 28 days curing (in water cabinet) then remained constant with time. The potentials of these electrodes in dry concrete containing 0 to 0.6% chloride was about -300 to -350 mv vs $Cu/CuSO_4$ and remained constant with time. However, the potentials of these electrodes in concrete containing 1.2 and 2.1% Cl^- ion remained constant at the potentials about -400 to -450 mv, respectively. An increase of 100 to 150 mv in potential may be to some degree related to the differences in the IR drop between Mo/MoO_3 and $Cu/CuSO_4$ because an increase in the chloride content of concrete will decrease the resistivity of concrete as reported (25). The potential shift in concrete after 28 days raises some interesting questions. Experiments by Hammond and Roberson (26) and Monfore (27) support the view that conduction is by means of ions in the evaporable water in the cement paste, the principal ions being Ca^{++}, Na^+, K^+, OH^-, and SO_4-- (28). Since the amount of evaporable water in a typical cement paste varies from approximately 60% by volume at the time of mixing to 20% after full hydration (29), the electrical conductivity of concrete should also be a function of time.

Therefore, it is clear that an increase in the resistivity of concrete due to the gradual evaporation of water from concrete results in a higher IR drop between Mo/MoO_3 and $Cu/CuSO_4$ and thus causes a potential shift to occur.

In water saturated concrete there was no shift in the potential of embedded Mo/MoO_3 electrodes after curing, and the potential of these electrodes remained constant with time. This is indicative of the fact that in water saturated concrete, since there is no loss of water in concrete with time, the resistivity of concrete remains the same; therefore, the potential of the electrodes will stay constant with time. It was observed that any variable that can influence the resistivity of concrete will affect the potential of Mo/MoO_3 with respect to $Cu/CuSO_4$. For instance, an increase in the chloride level of concrete increased the potential of these electrodes due to the decrease in the resistivity of concrete.

In order to further investigate the effect of IR drop on the potential measurements of Mo/MoO_3 vs $Cu/CuSO_4$ electrode, a 0.1% chloride contaminated concrete cylinder containing a batch of five Mo/MoO_3 electrodes which had been in the laboratory dry condition for five years was used. The potential of the Mo/MoO_3 electrodes vs $Cu/CuSO_4$ as a function of distance was measured in this cylinder. It was observed

that the potential between $Cu/CuSO_4$ and Mo/MoO_3 electrodes shifted significantly toward a more positive value with an increase in distance between the electrodes. The cylinder was soaked in distilled water for two weeks and the potential of Mo/MoO_3 electrodes vs $Cu/CuSO_4$ shifted toward more negative values of -550 to -600 mv. The potentials remained constant with time and there was no change on the potential as the distance between Cu/CuSO and Mo/MoO_3 electrodes increased. The reduction in the resistivity of concrete (dry concrete - 10^8 - 10^9 ohm-cm, water saturated concrete 10^3 - 10^4 ohm-cm) reduced the IR drop and shifted the potential toward more negative value. Harco (30) has developed a technique for obtaining valid and accurate pipe-to-soil potential measurements on pipelines which were under paved areas such as concrete or asphalt runways. This study indicated that when the potential of the pipe was measured with the reference electrode located on an unpaved grassy area, six inches away from the pipe, the potential was about 300 mv less negative than that when the reference electrode was placed on concrete two inches from the pipe. In addition, in experiments conducted on concrete slabs 2' x 2' x 2' in the laboratory they found that the potential of rebar vs $Cu/CuSO_4$ was about -485 to -535 mv. However, when water was poured onto the slabs the

potentials measured from on the concrete became more negative. In one test, they found that the potential increased to a value of -790 mv immediately after pouring water on the concrete and increased to a value of -850 mv after 15 minutes. The results found by Harco are in good agreement with the findings in this project which indicated that the contact point between $Cu/CuSO_4$ and concrete and the resistivity of concrete will influence the potential measurements of embedded Mo/MoO_3 and rebar. Therefore, based on the results found in this project, it seems that Mo/MoO_3 electrode is a rugged reference electrode with a stable potential. The variations of the potential of Mo/MoO_3 electrode vs $Cu/CuSO_4$ are not related to a defect or poor performance of these electrodes but rather to the effect of IR drop developed between Mo/MoO_3 and an external $Cu/CuSO_4$. If these electrodes are embedded adjacent to the reinforced steel structures, the true value of the potential may be determined which leads to a correct anticipation of the corrosion initiation of the reinforced structures. However, a correct criterion for potential of the reinforced steel vs Mo/MoO_3 must be developed to indicate at what potentials the rebar are not corroding as this has been the case for $Cu/CuSO_4$.

The use of eight Mo/MoO_3 electrodes in a bridge deck located on Highway 51 (Payne County) demonstrated that

the potential of these electrodes 9-10 months after installation are in the range of -170 to -370 mv vs $Cu/CuSO_4$ electrode. The 200 mv variation in the potential may be due to the differences of the distance between Mo/MoO_3 electrodes and $Cu/CuSO_4$ since the Mo/MoO_3 electrodes were embedded in different locations throughout the bridge.

Effect of Long Term Current Tests

Based on the findings in this study, the cathodic current in the magnitude of 3 ma/ft^2 (based on the surface area of rebar) will reduce the bond strength between rebar and concrete after two years of exposure to the impressed current. The 3 ma/ft^2 of cathodic current shifted the steel potential to the ranges of -680 to -780 mv with respect to $Cu/CuSO_4$. These potentials were well below the hydrogen generation potential which might cause a bond failure between the rebar and concrete.

The pull-out strength data are very scattered as shown by the large standard deviations (up to 20.2% fractional standard deviation). This provides some difficulty in making definite conclusions from the results. However, the data at five years do indicate with a high degree of certainty that differences in pull-out strength are significant. The mean pull-out strength decreased by 21.3%. There is a 94.5% certainty that the true values of the means differ at least as much as 6% and as much as 34.5%. (These were obtained by using the minimum and maximum differences between the means $\pm \sigma_m$.)

This study did not have as a purpose to evaluate the significance of a 20-30% drop in pull-out strength on the performance of a reinforced concrete structure. There should be a concern, however, with use of cathodic protection over time periods longer than five years. It is possible the bond strength could continue to drop and at some time reach a level at which the structural integrity might be doubtful. Studies for longer than five years should be initiated to confirm or repudiate the results presented in this work.

Visual inspection of the rebars and concrete at the regions around the rebar after the pull out strength test showed that for a period up to 42 months of exposure there was no sign of pitting on the rebar surface for both the test and the control specimen. However, after 42 months of exposure pitting was found on some of the rebars from the control cylinders but there was little indication of pitting on the rebars from the specimens subjected to impressed currents.

There was some evidence of a different failure mode in the pullout strength tests between the cylinders exposed to current and the control cylinders. This difference was seen on the samples after 4 years or more of current exposure. The failure of the samples from the control batch seemed to occur most often at the rebar concrete interface. Most of the rebars taken from the control cylinders were bare while the rebars from the cylinders exposed to current had concrete adhering to them after pull-out tests were made. In addition, the failure mode seemed to be in the concrete matrix rather than at the rebar-concrete interface.

Casad (7) observed a similar sort of difference in testing done at much higher current densities (10^2-10^3 ma/ft^2). In addition he observed that the concrete seemed to have softened after exposure to the high cathodic currents. There was some indication in this work that the concrete was softened in the samples exposed to current. However, this observation was difficult to quantify and is a bit subjective.

The chemical analysis of sodium (Na^+) and potassium ions (K^+) for the specimen subjected to the impressed current indicated a build up of Na^+ and K^+ ions at the regions near the rebar is due to ionic migration which takes place between anode and cathode. However, the chemical analysis of sodium and potassium ions in the control cylinders showed that these cations moved away from the regions near the rebar toward the concrete surface with time. The migration of the ions from the regions near the rebar toward the concrete surface in the control specimen is probably due to the evaporation of the water from the concrete which carries the ions toward the concrete surface.

Considering both the weakening of the bond between the rebar and concrete and the buildup of the sodium (Na^+) and potassium (K^+) ions at the regions near the rebar for the specimen subjected to the impressed current, it appears that the softening of the concrete near the rebar may be due to the buildup of Na^+ and K^+ ions. The hydroxides of these ions are believed to attack the calcium and aluminosilicate thus producing soluble silicates which in turn contribute to the softening of the concrete. These findings are in line with

the experimental studies of the National Bureau of Standards (8) who tested concrete blocks subjected to very high cathodic current for relatively short period of time. The National Bureau of Standards also found that the comparison between the test and the control cylinders in some cases indicated a loss of approximately 80% of the original bond strength for the test specimens. This was thought to be due to the buildup of Na^+ and K^+ ions in regions near the rebar.

In addition to the chemical analysis for Na^+ and K^+ ions, the chloride analysis was run to investigate the effect of the impressed current on the Cl^- ions. All of the specimens under the experiment had originally 0.1% NaCl (0.06% Cl^-). It was found that the Cl^- ions in the specimen moved away from the region near the rebar toward the concrete surface. The anions (Cl^-) in the concrete move towards the positively charge electrode (anode) and as a result the Cl^- ions will migrate toward the concrete surface.

In bridge decks an experimental technique has been used to remove the Cl^- from the deck. Of course, the magnitude of the current used for removing chloride from the deck is much higher than the current used in this study.

It is of interest to note that the Cl^- concentrations in the region near the rebar and the mid-section between the rebar and the concrete surface for the control specimens were about the same as the amount of Cl^- initially added to the specimen (0.06% Cl^-). The aggregate used in the mix also

contained a small amount of chloride. However, the chloride concentration at the concrete surface was lower than that at the region near the rebar. This effect is not clearly understood and may be due to the more complex reaction of Cl^- with the concrete matrix which occured at the concrete surface due to the higher availability of oxygen and carbon dioxide. This may cause some of the Cl^- to be bound with the concrete matrix in a manner that the method developed by Berman (13) can not detect some of the Cl^- ions.

CONCLUSIONS

Based on the findings in this project the following conclusions can be drawn:

1. It is possible to make an asphaltic concrete with sufficient conductivity and stability for a cathodic protection system overlay. A mix with 7-11% asphalt, 45% coke breeze and the remainder a standard aggregate has a resistivity of about 100 ohm-cm which is in the range needed for cathodic protection use. The Hveem stability was above 35 for each mix made to these proportions which is the minimum required by the Oklahoma Department of Transportation.
2. An increase in salt concentration of concrete from 0 to 0.1% did not increase the corrosion rate of steel in concrete drastically. However, corrosion rates of steel in concrete increased significantly with increases in salt concentration from 0.1 to 0.2% and from 0.2 to 0.5%.
3. The molybdenum/molybdenum oxide (Mo/MoO_3) electrode has been found to have good prospects for use as an imbeddable reference electrode in concrete. This electrode is physically rugged and has stable potential with respect to time.
4. Sodium and potassium ion concentrations at the regions near the rebar increased with time for the concrete specimen subjected to 3 ma/ft^2 cathodic impressed current. The chloride ions in these specimens, as expected, migrated away from the rebar regions toward the concrete surface.

5. An impressed current in magnitude equivalent to the level practiced in cathodic protection (3 ma/ft^2) caused a deterioration of concrete after about 3.5 years of exposure. The weakening of the bond between the rebar and concrete seemed to be due to the build up of sodium and potassium ions at the regions near the rebar. These results indicate there should be some concern about the long term effects of cathodic protection for reinforced concrete structures.

References

1. P.D. Cady, "Corrosion of Reinforcing Steel in Concrete - A General Overview of Problem" ASTM STP 629, pp. 3-11 (1977).

2. H.K. Cook and W.J. McCoy, "Influence of Chloride in Reinforced Concrete", ASTM STP 629, pp. 20-29 (1977).

3. W.R. Schutt, "Practical Experiences with Bridge Decks Cathodic Protection", Corrosion/78, Paper No. 74, NACE, Houston, Texas, 1978.

4. H.J. Fromm, "Cathodic Protection of Concrete Bridge Decks in Ontario", Corrosion/76, Paper No. 19, NACE, Houston, Texas, 1976.

5. "Salt Damaged Bridge Decks: Cathode Protection Helps", Civil Engineering - ASCE, Sept., 1975.

6. C.E. Locke, Specialized Studies - Cathodic Protection of Rebars in Bridge Decks, Report to ODOT, April 1976.

7. B.M. Casad, "The Effect of Cathodic Current on Bond Strength Between Concrete and Reinforcing Steel", MS Thesis, Oklahoma State University, August, 1951.

8. E.B. Rosa, B. McCollum and O.S. Petters, "Electrolysis of Concrete", Nat. Bur. Standards Technol. Paper No. 18, 1913.

9. Unpublished report from Rock Island Arsenal Corps of Engineers, 1953.

10. D.A. Hausmann, J. Am. Conc. Inst., 61 (2) 171 (1964).

11. J.B. Vrable, "Cathodic Protection for Reinforced Concrete Bridge Decks", Final Report, NCHRP Project 12-12, July 1974.

12. Perkin Elmer, Atomic Absorption Analysis Methods.

13. H.A. Berman, "Determination of Chloride in Hardened Portland Cement Paste, Mortar and Concrete", Report No. FHWA-RD-72-12. Federal Highway Administration, September 1972.

14. H.H. Uhlig, "Corrosion and Corrosion Control", 2nd Ed., John Wiley and Sons, New York, 1971.

15. R.L. Every and W.P. Banks, Corrosion, 23, 151 (1967).

16. P.K. Metha, ASTM STP 629, pp. 12-19 (1977).

17. M. Ben-yair, Cement and Concrete Research, Vol. 4, No. 3, pp. 405-416 (1974).

18. V.K. Gouda, M.A. Shater and R. Sch. Mikhail, Cement and Concrete Research, 5, 1 (1975).

19. S.N. Alekseev and N.K. Rozental, Protection of Metals, 536 (1975), Translated from Zaschitz Metal. 10 (5), 585 (1974).

20. D.F. Griffin and Henry, ASTM Proceeding 63, 1046 (1963).

21. D.A. Hausmann, Material Protection, Vol. 6, No. 11, pp. 12-23 (1967).

22. K.C. Clear, and R.E. Hay, Report No. FHWA-RD-73-32, Vol. 1, 1973.

23. D.J.G. Ives and G.J. Janz, Reference Electrodes, Academic Press, New York, (1961).

24. R.L. Henry, "Water Vapor Transmission and the Electrical Resistivity of Concrete", Port Hueneme, U.S. Naval Civil Engineering Laboratory, 25 June 1964. Technical Report R314.

25. E. Hammond and T.D. Robson, "Comparison of Electrical Properties of Various Cements and Concretes", The Engineers, Vol. 199, pp. 78-80, Jan. 1975.

26. G.E. Monfore, "The Electrical Resistivity of Concrete", Journal of the PCA Research and Development Laboratories, Vol. 10, No. 2, pp. 35-48, May 1968.

27. N. Aschan, "Determining the Setting Time of Cement Paste, Mortar and Concrete with a Copper-Lead Electrode", Magazine of Concrete Research, Vol. 18, No. 56, September 1968.

28. A.M. Neville, "Properties of Concrete", Second edition, London, Pitman Publishing, p. 29, 1973.

29. B. Husock, "The Effect of Paving on Pipe-to-Soil Potentials", Harco Corporation, Paper No. HC-45 presented at American Gas Association Distribution Conference, Hollywood, Florida, May 7-9, 1979.

APPENDIX

APPENDIX A

PROCEDURE FOR TOTAL CHLORIDE IN PORTLAND CEMENT AND CONCRETE

Apparatus

1. Combination chloride electrode model 96-17 with combination Cl^- electrode filling solution 90-00-17 was used. This electrode is the most convenient type which requires less maintenance than the single electrode or the membrane type.

2. A Keithly 620 electrometer.

3. Magnetic stirrer and teflon stirrer rod.

4. Burette with .05 ml graduations.

Test Procedure By Berman Method[13]

This method contains a procedure for total chloride content of dry or hydrated portland cement concrete. For simplicity, the procedure is outlined in different sections as follows. This method is valid only for the materials which do not contain sulfides, but the extraction procedure, Sections 1 and 2, may be used for all such materials.

1. Three gram powdered sample was weighed and 10 ml of distilled water was added, swirling to bring the powder into suspension. Then, 3 ml of concentrated HNO_3 was added with continued swirling until the cement is completely decomposed. Any lumps which may exist were broken up with a stirring rod and were diluted with hot water at 50 ml. The acidity of solution was checked with methyl orange indicator.

2. The acid solution or slurry was heated to boiling on a hot plate of heater at medium heat and was boiled for about one minute. Then, the solution was removed from the hot plate and filtered into a 250 ml beaker. The clear solution was decanted and the residue was washed in the beaker once, was then transferred into E-D filter paper grade size 11 cm with the aid of hot distilled water. The filter paper was thoroughly washed (5 to 10 times) with the hot water. Then, the filtrate was allowed to cool to room temperature.

3. The combination chloride ion electrode was filled with the solution orion 90-00-17 recommended by the manufacturer, was plugged into the Keithly 620 electrometer, and the approximate position of the equivalence point was determined by immersing the electrode in a beaker of distilled H_2O.

4. The beaker of distilled H_2O was removed. The electrode was wiped with absorbent paper, and the electrode was immersed in the sample solution. The volume of successive increments of the standard $AgNO_3$ solution from the burette (0.01 N or 0.25N, depending on the quantity of chloride expected) was added and recorded, recording the millivoltmeter reading after each addition. The increment of $AgNO_3$ solution should be enough to change the reading by 5 to 10 mv. As the titration proceeded, smaller increments of $AgNO_3$ solution were sufficient to deflect the needle by this amount, until increments of only 0.1 or even .05 ml were effective (starting about 40 mv from the equivalence point). After the equivalence point was

reached, the needle deflections began to decrease with equal increments of $AgNO_3$ solution. The end point of titration was considered as the midpoint of the increment which produced the largest deflection per unit of silver nitrate added and usually occurred near the approximate equivalence point of the electrode. The degree of asymmetry was used to establish the endpoint within 0.01 ml when the increments of $AgNO_3$ solution were 0.1 ml.

Calculation

The percent chloride in the sample = $\frac{35.453VN}{10W}$, where V stands for the volume of silver nitrate solution, in ml, added up to endpoint. N is the normality of the silver nitrate solution. W is the weight of the sample in grams. In this chloride analysis the effect of moisture in sample and also preventing aggregate induced distortions were not considered.

Water Soluble Method

This method was modified by Berman method.[13] In this method instead of HNO_3, distilled water was used.

Procedure for Sodium and Potassium Ionic Analysis

The procedure described here was taken from the standard analyses provided by Perkin Elmer (12).

POTASSIUM IN CEMENT

SCOPE

This method provides for the determination of potassium in cement in the range from 0.2 to 1%.

REAGENTS

Concentrated hydrochloric acid

Potassium chloride or potassium nitrate

STANDARD SOLUTIONS

Stock Solution - Make up one liter of a 100µ/ml potassium solution as the chloride or nitrate.

Working Standards - Prepare 50-ml solutions containing 2.0, 4.0, 6, 8, and 10 µg/ml potassium. If an accuracy of better than 10% of the amount present is required, calcium chloride should be added to the standards approximately in the same concentration as will be present in the sample solutions.

OPERATING CONDITIONS

See Standard Conditions for Potassium (K 1). The use of recorder readout is recommended.

SAMPLE PREPARATION

Accurately weigh one gram of the sample, transfer to a 200-ml evaporating dish, moisten with 10 ml of cold water, and swirl. Add 10 ml of concentrated HCl and digest with gentle heat and agitation until solution is complete. Evaporate to dryness under an infrared heat lamp. Add 10 ml of 1:1 HCl, cover the dish, allow to stand for ten minutes, and add 10 ml of hot water. Filter through Whatman No. 541 paper or the equivalent

volumetric flask and dilute to the mark. The analyses are run on a ten-times dilution of this solution.

SODIUM IN CEMENT

SCOPE

This method provides for the determination of sodium in cement in the range from 0.05 to 0.5%. For higher sodium concentrations, further dilution is required.

REAGENTS

Concentrated hydrochloric acid

Sodium chloride or sodium nitrate

STANDARD SOLUTIONS

Stock Solution - Make up one liter of a 1000-µg/ml sodium solution as the chloride or nitrate.

Working Standards - Prepare 50-ml solutions containing 1, 2, 4, 6, 8 and 10 µg/ml sodium. If an accuracy of better than 10% of the amount present is required, calcium chloride should be added to the standards approximately in the same concentration as will be present in the sample solutions.

OPERATING CONDITIONS

See Standard Conditions for Sodium (Na 1). The use of recorder readout is recommended.

SAMPLE PREPARATION

Accurately weigh one gram of the sample, transfer to a 200-ml evaporating dish, moisten with 10 ml of cold water, and swirl. Add 10 ml of concentrated HCl and digest with gentle heat and agitation until solution is complete. Evaporate to dryness under an infrared heat lamp. Add 10 ml of 1:1 HCl, cover the dish,

allow to stand for ten minutes, and add 10 ml of hot water Filter through Whatman No. 541 paper or the equivalent and wash with ho 1:99 HCl. Transfer the filtrate to a 100-ml volumetric flask and dilute to the mark. The analyses are run on a ten-times dilution of this solution.

ANALYSIS

A Model 303 Atomic Absorption Spectrophotometry was used for the analysis of the sample and standard solution. A potassium and sodium hollow cathode lamp was used to provide narrow line spectra.

After preparation of the sample and standard solutions of potassium and sodium as described in the previous sections, the percent absorbance values for the sample and standard solutions were determined. Normally, standards were analyzed at the beginning and end of a run. Then the percent absorption was converted to the values of absorbance from the conversion table (Model 303). A plot of absorbance versus the concentration of the standard solutions of potassium and sodium was made. This plot gives a known concentration curve. The concentration of the sample solutions of potassium and sodium were determined at the point where the absorbance of the sample solution intercepts the concentration curve. Then the concentration of sodium and potassium in the sample solutions were converted to the concentrations of these ions in concrete. The detailed procedures are given in Perkin Elmer book (12).

Table 1

Matrix of Mixes showing the number of samples made for each combination using the graded coke-breeze

% AC / % Coke Breeze	5	7	9	11	13
15	3	3	3	3	N.G.
25	N.G.	3	3	3	N.G.
35	N.G.	3	3	3	N.G.
45	N.G.	3	3	3	3
55	N.G.	N.G.	3	3	3

Table 2

Concrete Mix Design (Class AA)*

Components	Weight % (Dry Basis)
Cement	16.8
Coarse Aggregate	51.2
Fine Aggregate	32.0
Water/Cement Ratio	0.45

*Class AA mix specified by the Oklahoma Department of Transportation.

Table 3

A Typical Data Sheet, showing aggregate and coke-breeze calculation for mixes

25% Coke-Breeze

Project No. 158-626

Test performed by Basden & Bliss,

at ODOT.

Date of:

a) Compaction 7-12-77 b) Stability Test 7-19-77

Total Sample Wt. 665 g.

% Aggregate=100-% Coke-Breeze = 75

% Rock	0.75(13)=9.75
% Screenings	0.75(65)=48.75
% Sand	0.75(22)=16.5

Calculation of Aggregate Wts.:

0.0975 x 665 =	64.8	g Rock
0.4875 x 665 =	324.2	g Scr.
0.165 x 665 =	109.7	g Sard
0.25 x 665 =	166.3	g C.S.

Calculation of Asphalt Wts.:

5% AC: $W_a=0.05\ (W_a +\ \ )$	W_a =	g
7% AC: $W_a=0.07\ (W_a + 665)$	W_a = 50.1	g
9% AC: $W_a=0.09\ (W_a + 665)$	W_a = 65.8	g
11% AC: $W_a=0.11\ (W_a + 665)$	W_a = 82.2	g
13% AC: $W_a=0.13\ (W_a + 665)$	W_a = 99.4	g

Remarks: Sampe wt. of 665 g. was obtained by a linear interpolation of 15g. per 1/32, based on coke-breeze percentages. 5% AC was abandoned since it was too dry on the 15% C.B. samples.

Table 4

Corrosion Rates of Reinforcing Steel

in Laboratory-dry Concrete

NaCl Wt%	Rate of Corrosion (MPY)	Corrosion Rate by Petrolite Model M-1013 instrument (MPY)
0	0.024	0.003
0.05	0.027	0.003
0.08	0.024	0.005
0.1	0.030	0.006
0.2	0.367	0.07
0.5	1.06	0.2
1	6.49	0.52

TABLE 5
Potentials of Ag/AgCl in Solution
Compared to Saturated Calomel

SALT Soln:

Cl^- Content, wt%	Potential, mv	Standard Deviation σ
0.25	38	6
0.50	28	3
1.0	17	4

Measured in $Ca(OH)_2$ Soln's

Cl^- Content	Potential, mv	σ
0.25	28	7
0.5	17	4
1.0	1	4

Stored and Measured in $Ca(OH)_2$

Cl^- Content	Potential, mv	σ
0.25	64	7
0.50	40	4
1.0	30	8

TABLE 6
Theoretical Potential of Ag/AgCl
Compared to Saturated Calomel

Cl^- Conc, wt %	Theor. Pot.
0.25	66 mv
0.5	49
1.0	33

TABLE 7

Potential of Ag/AgCl Electrodes Imbedded in Concrete Compared Saturated $Cu/CuSO_4$

Cl^-, wt%	Potential, mv
0.1	68
0.2	26
0.5	10

TABLE 8

Potential of Mo/MOO_3 in dry Concrete Compared to $Cu/CuSO_4$

Cl^- wt.%	Average Potential, mv	Standard Deviation, mv
0	309	15.6
0.1	262	17.7
0.2	267	10.7
0.5	294	10.6

TABLE 9

Potential of Mo/MoO_3 vs. Electrodes in Water-Saturated Concrete VS $Cu/CuSo_4$ as a Function of Cl^- Concentration

Samples had been exposed to distilled water for 30 days after 5 days of curing.

% Cl^- Mixed with Concrete	Potential Mo/MoO_3 VS $Cu/CuSo_4$ MV
0	-520
0.06	-530
0.3	-550
0.6	-630
1.2	-660
2.1	-800

Table 10

Potential of Mo/MoO_3 electrodes in the five years laboratory dry concrete containing 0.1% Cl^-.

Electrode No.	Potential measured at a distance of 1 inch from $Cu/CuSO_4$.	Potential measured at a distance of 3 inches from $Cu/CuSO_4$.
1	-285	-89
2	-260	-100
3	-250	-105
4	-270	-79
5	-220	-92

Table 11

Potential of Mo/MoO_3 electrodes in the same concrete cylinder as in Table 8 after two weeks of exposure to distilled water.

Electrode No.	Potential measured at a distance of 1 inch from $Cu/CuSO_4$	Potential measured at a distance of 3 inches from $Cu/CuSO_4$
1	-640	-647
2	-602	-598
3	-587	-598
4	-583	-591
5	-585	-546

TABLE 12 ACCEPTABLE MIX DESIGNS

Type of Mix Based on Asphalt %	Coke Breeze %	Optimum Mix		
		Coke Breeze %	ρ ohm-cm	R Hveem stability
7	15, 25, 35, 45	35	35	37
9	35, 45	45	60	38
11	35, 45, 55	45	60	38

Table 13

Year 1

Pullout Strengths
in pounds force per square inch, psi

	Control	Batch -No-	CP
3 MO	19900	1	16700
	18250		18100
	19600		19800
	21350		15800
6 MO	19100	5	12550
	17600		16500
	15450		18150
	14200		16000
9 MO	17025	1	19925
	17150		16625
	17150		17075
	17375		14950
12 MO	20500	5	16800
	16600		18050
	15850		17875
	16800		21700
Mean $\tilde{x}$ =	17744	Mean $\tilde{x}$ =	17288
σ =	1867	σ =	2070
σ_m =	466	σ_m =	517
FSD =	10.6%	FSD =	11.9%

σ = std dev. = $\sqrt{\frac{(\tilde{x}-x_i)^2}{n}}$

σ_m = std error of mean = $\frac{\sigma}{\sqrt{n}}$

Frac. std. Deviation = $\frac{\sigma_m}{\tilde{x}} \times 100$

Table 14

Year 2

Pullout Strengths
in pounds force per square inch, psi

	Control	Batch -No-	CP
15 MO	18850	1	16850
	17550		19900
	21500		16750
	21000		16525
18 MO	19600	5	13875
	18550		18400
	14600		18100
	17700		22950
21 MO	13050	2	18150
	16700		16800
	20200		14400
	15150		20100
24 MO	15250	6	16600
	16850		16150
	14650		16950
	18750		14400
Mean $\tilde{x}$ =	17497		17306
σ =	2404		2249
σ_m =	601		562
FSD =	13.7%		13.0%

σ = std dev. = $\sqrt{\frac{(\tilde{x}-x_i)^2}{n}}$

σ_m = std error of mean = $\frac{\sigma}{\sqrt{n}}$

Frac. std. Deviation = $\frac{\sigma_m}{\tilde{x}} \times 100$

Table 15

Year 3

	Control	Batch -No-	CP
27 MO	23300	2	18850
	17000		19550
	17300		20300
	17200		21600
30 MO	17350	6	19400
	19750		21100
	22800		16700
	20100		19000
33 MO	18350	3	20150
	21850		16250
	17900		18200
	18050		16550
36 MO	14300	7	11250
	16250		12750
	16750		15350
	10850		11650
Mean $\tilde{x}$ =	18069	Mean $\tilde{x}$ =	17416
σ =	3015	σ =	3167
σ_m =	754	σ_m =	792
FSD =	16.7%	FSD =	18.2%

σ = std dev. = $\sqrt{\frac{(\tilde{x}-x_i)^2}{n}}$

σ_m = std error of mean = $\frac{\sigma}{\sqrt{n}}$

Frac. std. Deviation = $\frac{\sigma_m}{\tilde{x}} \times 100$

Table 16

Year 4

	Control	Batch -No-	CP
39 MO	15650	3	16450
	20900		14650
	21350		17100
	21850		19100
42 MO	17750	7	19800
	20500		22250
	19250		17750
	14900		21150
45 MO	16450	3	10100
	18850		13450
	19450		17400
	21450		14500
48 MO	18950	7	19600
	19050		16750
	17900		12500
	22150		16050
Mean $\tilde{x}$ =	19150		16784
σ =	2131		3136
σ_m =	533		784
FSD =	11.1%		18.7%

σ = std dev. = $\sqrt{\frac{(\tilde{x}-x_i)^2}{n}}$

= std error of mean = $\frac{\sigma}{\sqrt{n}}$

Frac. std. Deviation = $\frac{\sigma_m}{\tilde{x}} \times 100$

Table 17

Year 5

	Control	Batch -No-	CP
51 MO	18850	4	17950
	17200		11050
	23000		13650
	21850		11600
54 MO	18800	8	19900
	17500		14200
	18000		19500
			19100
57 MO	20300	4	13800
	21500		13700
	22750		12450
	19300		13300
60 MO	23250	8	18200
	21400		18900
	23750		13050
	10650		20000
Mean $\tilde{x}$ =	19873		15647
σ =	3240		3157
σ_m =	810		789
FSD =	16.3%		20.2%

σ = std dev. = $\sqrt{\frac{(\tilde{x}-x_i)^2}{n}}$

σ_m = std error of mean = $\frac{\sigma}{\sqrt{n}}$

Frac. std. Deviation = $\frac{\sigma_m}{\tilde{x}} \times 100$

Table 18

Mean Pullout Strengths
by Year and Batch Number

Batch No	Yr (set)	Control	CP
1	1 (1)	19975	17600
1	1 (3)	17175	17143
1/2	2 (5)	19725	17506
2	2 (7)	16275	17362
2	3 (9)	20075	18875
3	3 (11)	19038	17788
3	4 (13)	19931	16825
3/4	4 (15)	19050	13862
4	5 (17)	20225	13562
4	5 (19)	20975	13312
5	1 (2)	16587	15800
5	1 (4)	17437	18606
5/6	2 (6)	17612	18331
6	2 (8)	16375	16025
6	3 (10)	20000	19050
7	3 (12)	14537	12750
7	4 (14)	18100	20237
7/8	4 (16)	19512	16225
8	5 (18)	18,100	18175
8	5 (20)	22,300	16200

Table 19

Mean Pullout Strength
for Each Set, psi

Set No.		Control			CP		
	Mo.	Mean	σ	σ_m	Mean	σ	σ_m
1	3	19975	1101	550	17600	1511	756
2	6	16537	1893	947	15800	2038	1019
3	9	17175	126	61	17143	1790	895
4	12	17437	1803	901	18606	1849	925
5	15	19725	1387	693	17506	1387	694
6	18	17612	1864	932	18331	3211	1606
7	21	16275	2610	1305	17362	2074	1037
8	24	16375	1590	795	16025	980	490
9	27	20075	1019	509	18875	2562	1286
10	30	20000	1932	866	19050	1569	785
11	33	19038	1632	816	17738	1552	776
12	36	14537	2317	1158	12750	1599	800
13	39	19931	2494	1247	16825	1590	795
14	42	18100	2088	1044	20237	1678	839
15	45	19050	1783	842	13862	2610	1305
16	48	19512	1588	794	16225	2528	1764
17	51	20225	2312	1156	13562	2712	1356
18	54	18100	535	168	18175	2312	1656
19	57	20975	1298	629	13312	532	266
20	60	19512	1587	794	17537	2669	1335

$$\tilde{x} = \frac{\Sigma x_i}{n}$$

$$\sigma = \sqrt{\frac{(\tilde{x}-x_i)^2}{n}}$$

$$\sigma_m = \frac{\sigma}{\sqrt{n}}$$

Table 20

Average Pullout Strength of
All Cylinders Pulled in One Year, psi

[Standard Deviation, Standard Error of Mean, and Fractional Standard Deviation also shown]

	Control				Current			
Year	Pullout, psi	σ	σ_m	FSD, %	Pullout, psi	σ	σ_m	FSD, %
1	17744	1867	466	10.6	17288	2070	517	11.9
2	17497	2404	601	13.7	17306	2249	562	13
3	13669	3015	754	16.7	17416	3167	792	18.2
4	19150	2131	533	11.1	16784	3136	784	18.7
5	19873	3240	810	16.3	15647	3157	789	20.2

$$\sigma = \sqrt{\frac{(\tilde{x}-x_i)^2}{n}}$$

$$\tilde{x} = \text{Mean} = \frac{\Sigma \tilde{x}_i}{n}$$

$$\sigma_m = \frac{\sigma}{\sqrt{n}}$$

$$\text{FSD} = \frac{\sigma_m}{\tilde{x}} \times 100$$

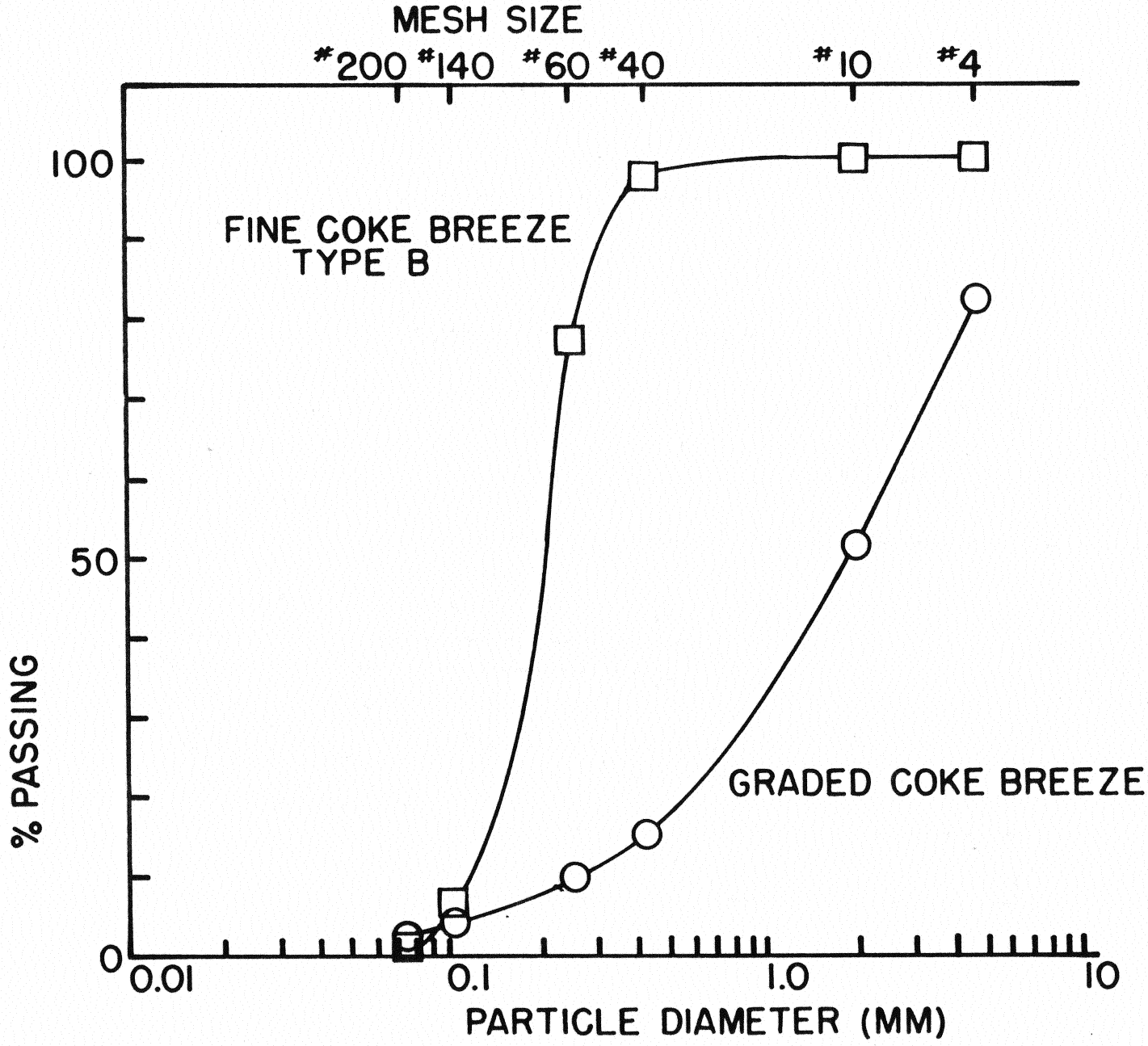
MESH SIZE
#200 #140 #60 #40 #10 #4
100
50
0
% PASSING
FINE COKE BREEZE
TYPE B
GRADED COKE BREEZE
0.01
0.1
1.0
10
PARTICLE DIAMETER (MM)

Figure 1

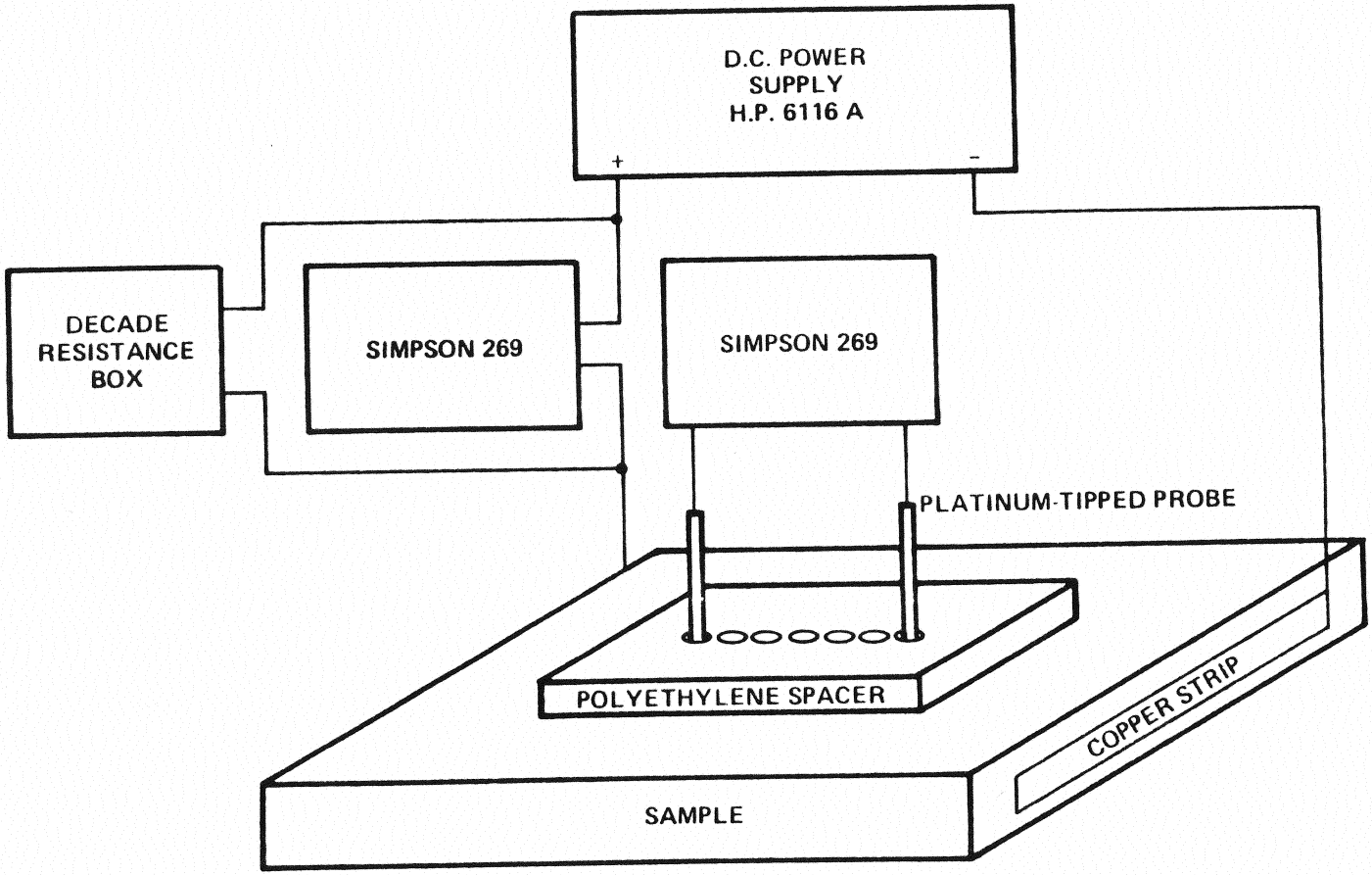

FIGURE 2 RESISTIVITY APPARATUS

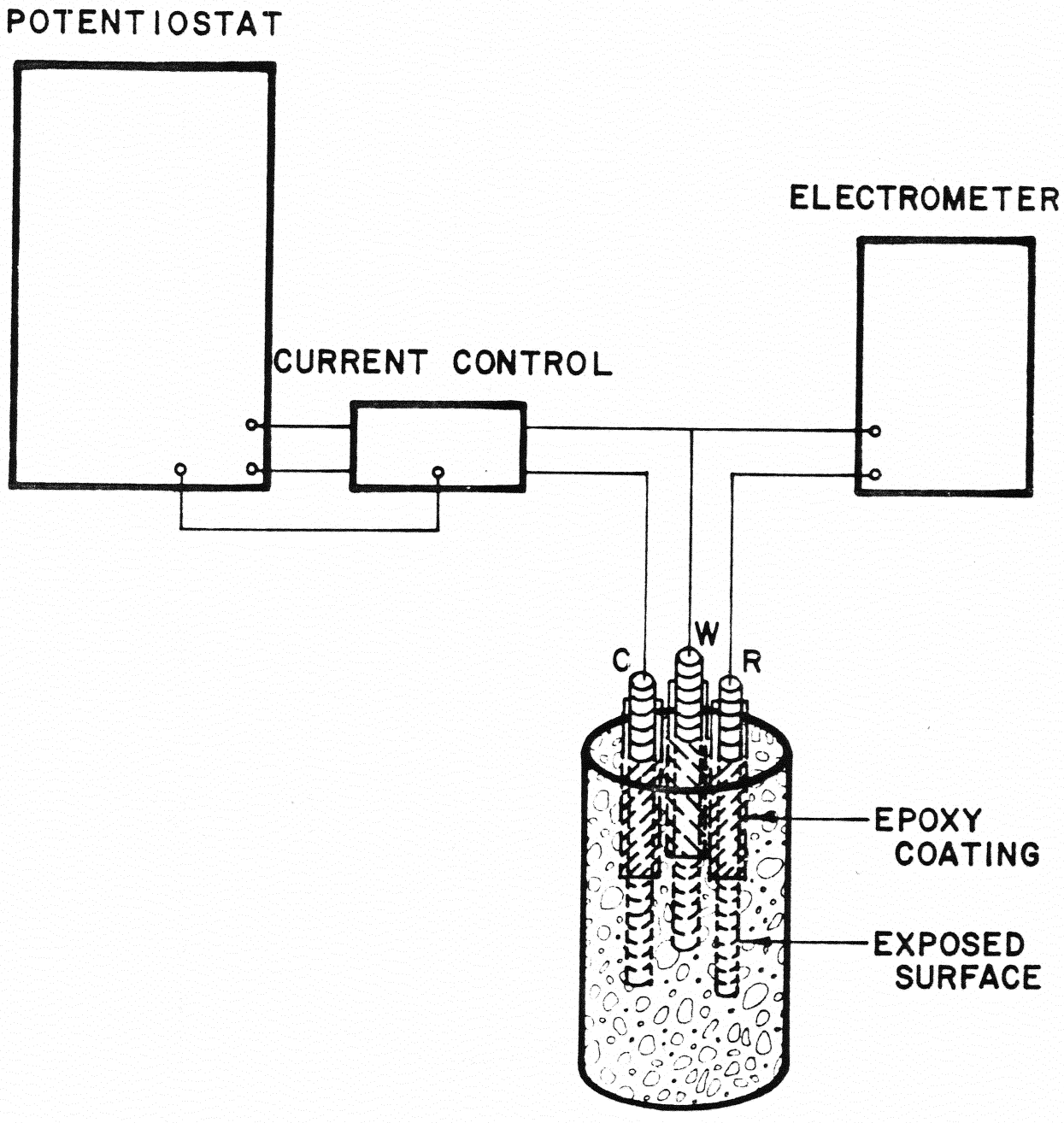

GALVANOSTATIC POIARIZATION SET UP USING REBARS AS REFERENCE, WORKING AND COUNTER ELECTRODE.

Fig. 3

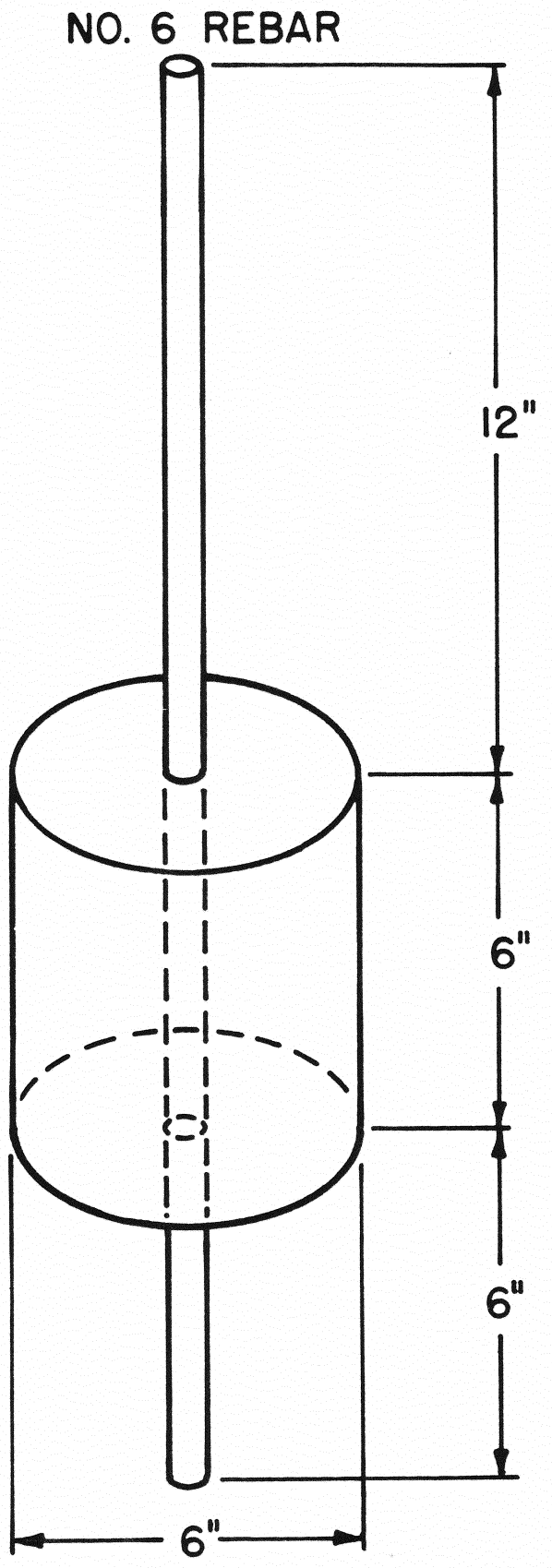

FIG. 4- CONCRETE CYLINDER CONFIGURATION USED FOR REBAR PULL OUT STRENGTH TEST

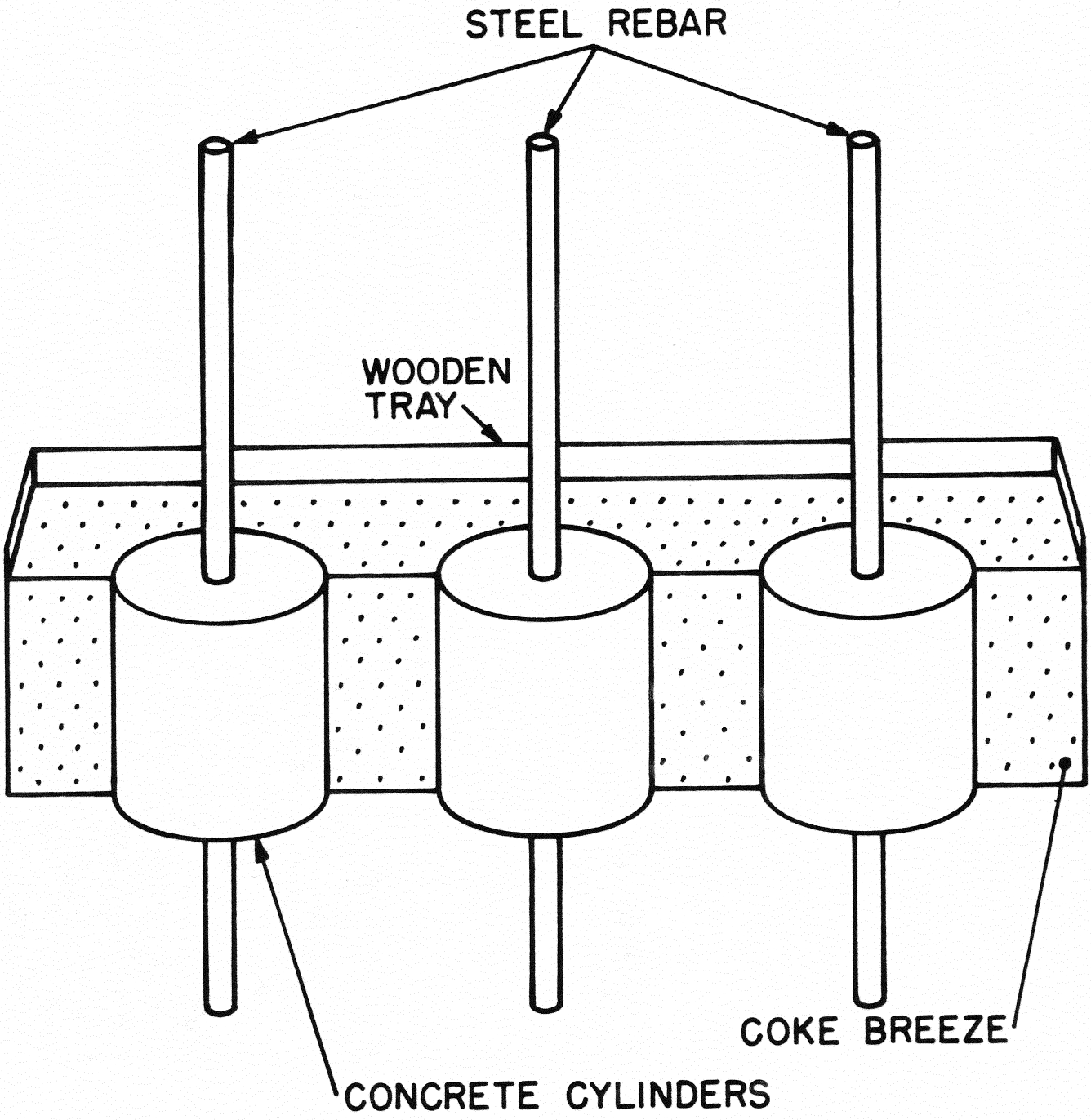

FIG. 5 - PLACEMENT OF CONCRETE CYLINDERS IN WOODEN TRAY CONTAINING COKE BREEZE

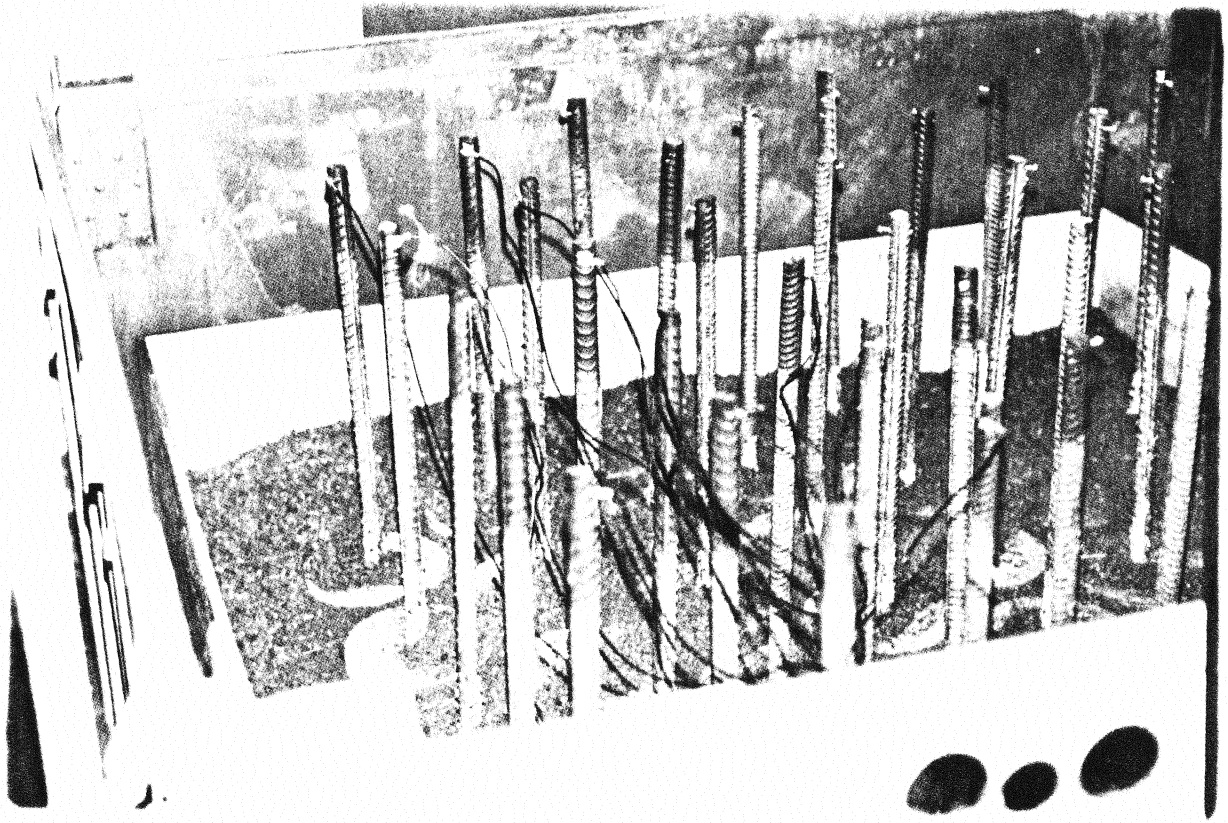

Fig. 6 - Spacing and the Placement of
Concrete Cylinders and Anodes in
Wooden Tray Inside the Sealed Box

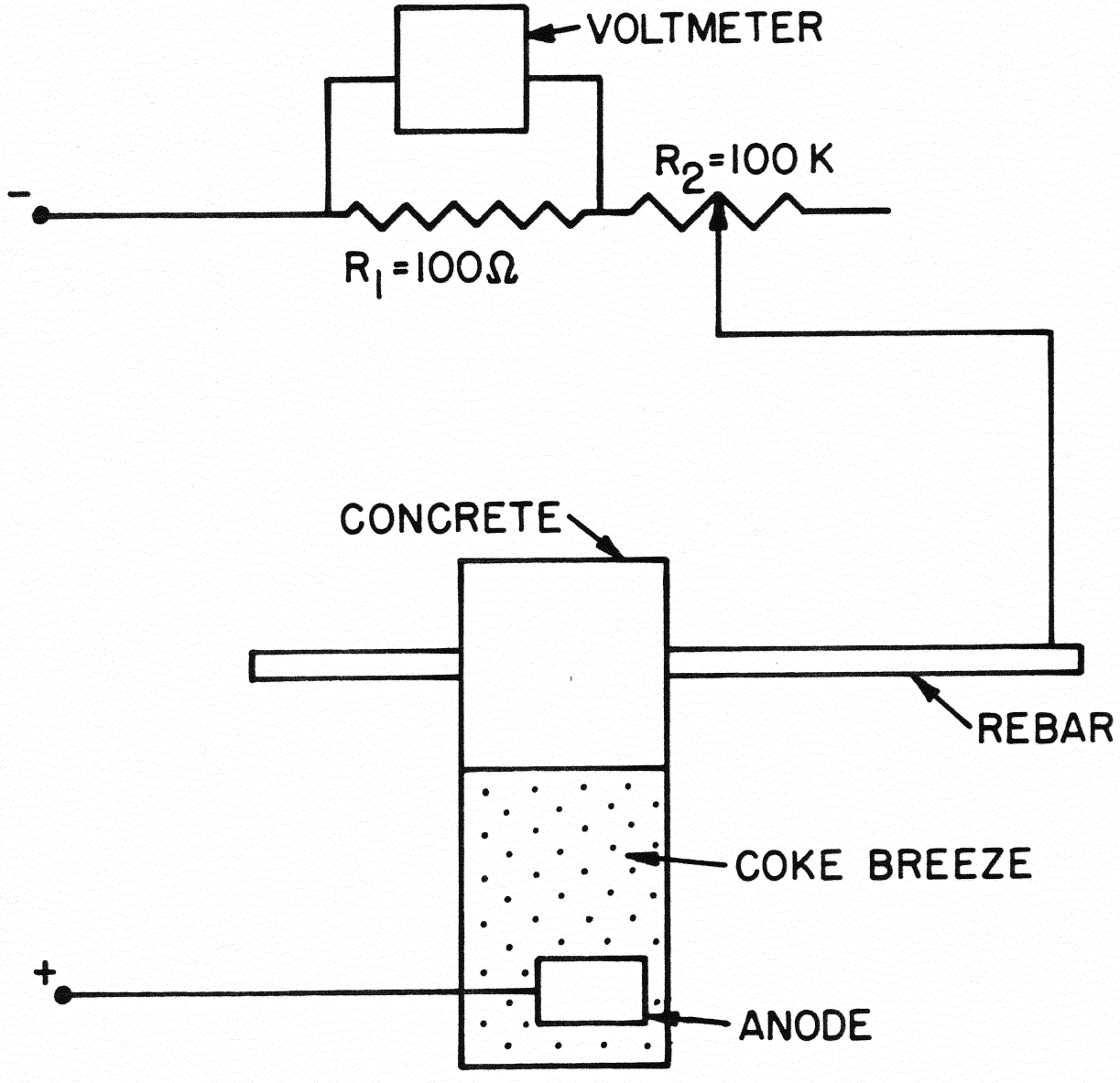

FIG. 7 - THE CURRENT TEST APPARATUS USED FOR CONTROL AND MEASUREMENT OF CURRENT THROUGH EACH REBAR

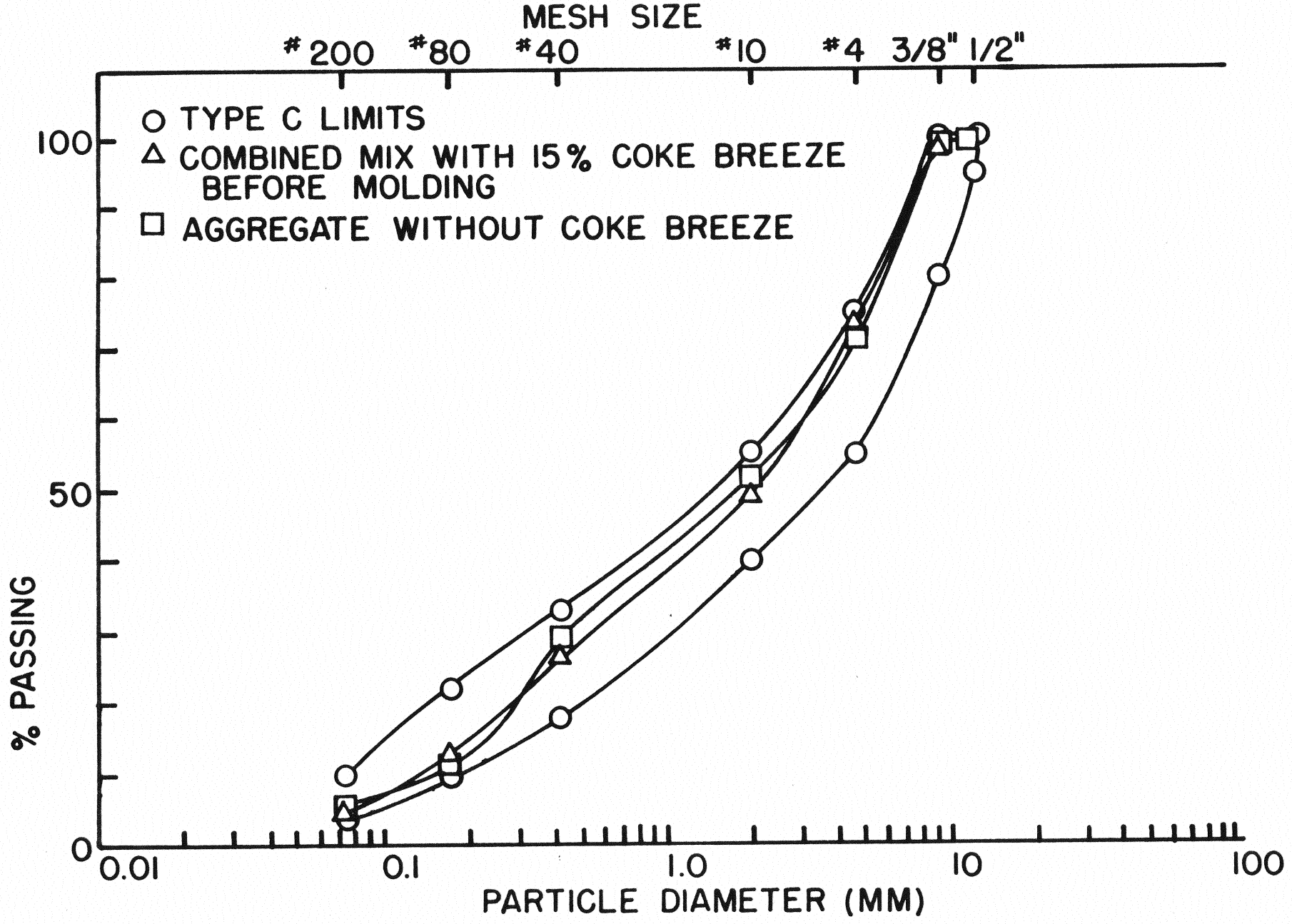
MESH SIZE
#200
#80
#40
#10
#4
3/8"
1/2"
TYPE C LIMITS
COMBINED MIX WITH 15% COKE BREEZE BEFORE MOLDING
AGGREGATE WITHOUT COKE BREEZE
100
50
0
% PASSING
0.01
0.1
1.0
10
100
PARTICLE DIAMETER (MM)

FIG. 8

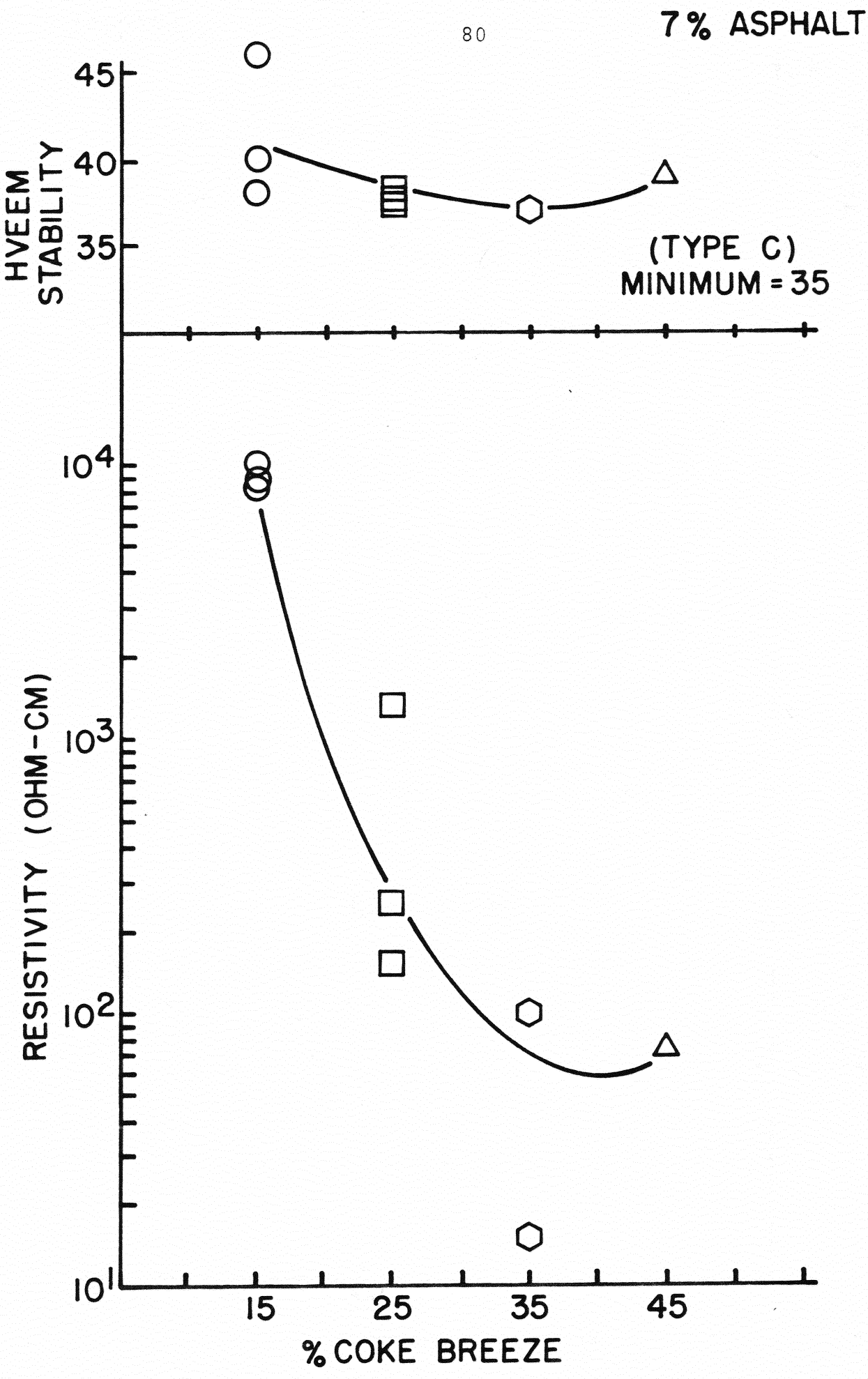
7% ASPHALT
HVEEM STABILITY
45
40
35
(TYPE C)
MINIMUM = 35
RESISTIVITY (OHM-CM)
10^4
10^3
10^2
10^1
15
25
35
45
% COKE BREEZE

FIG. 9

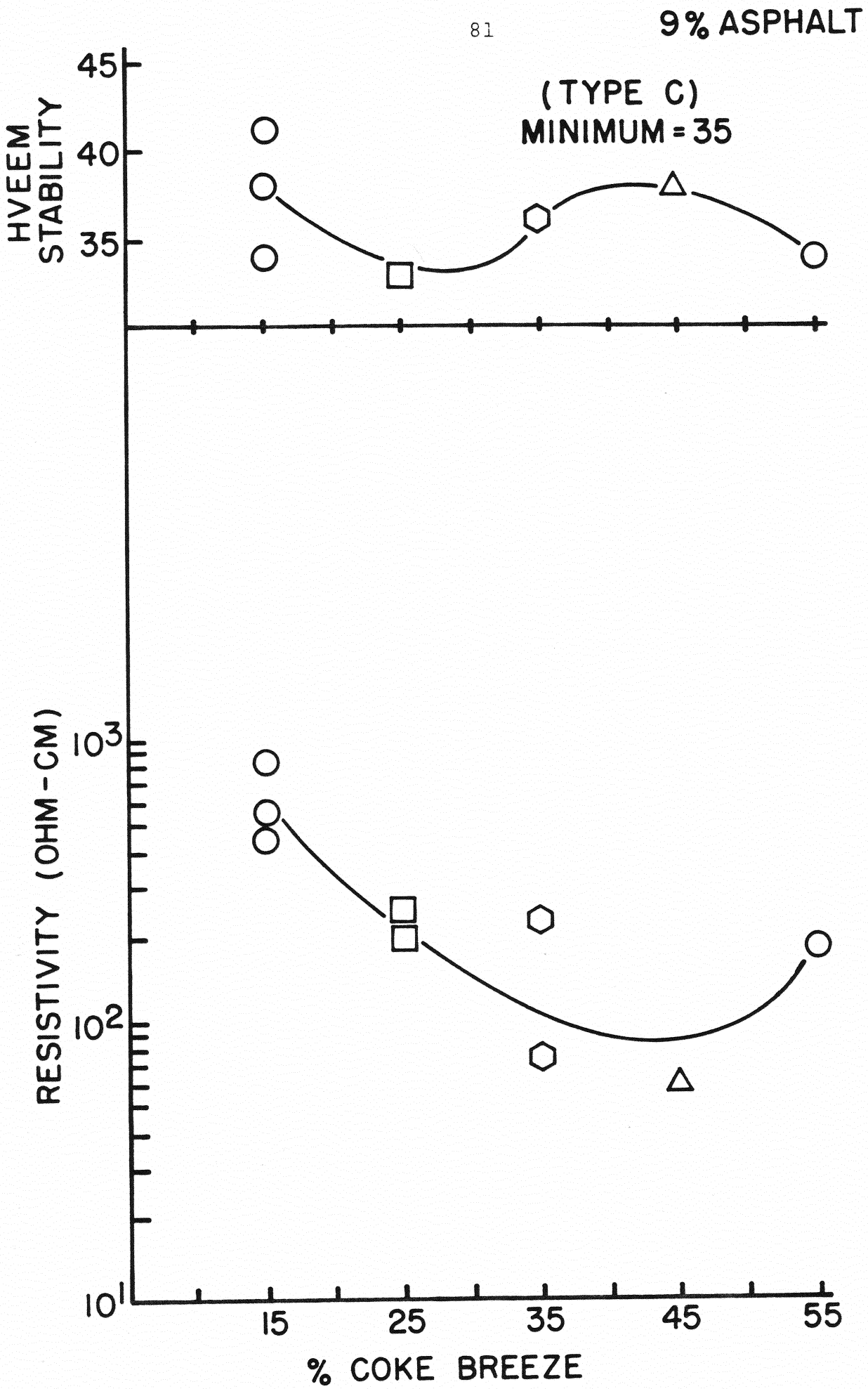
9% ASPHALT
(TYPE C)
MINIMUM = 35
HVEEM STABILITY
45
40
35
RESISTIVITY (OHM-CM)
10^3
10^2
10^1
15
25
35
45
55
% COKE BREEZE

FIG. 10

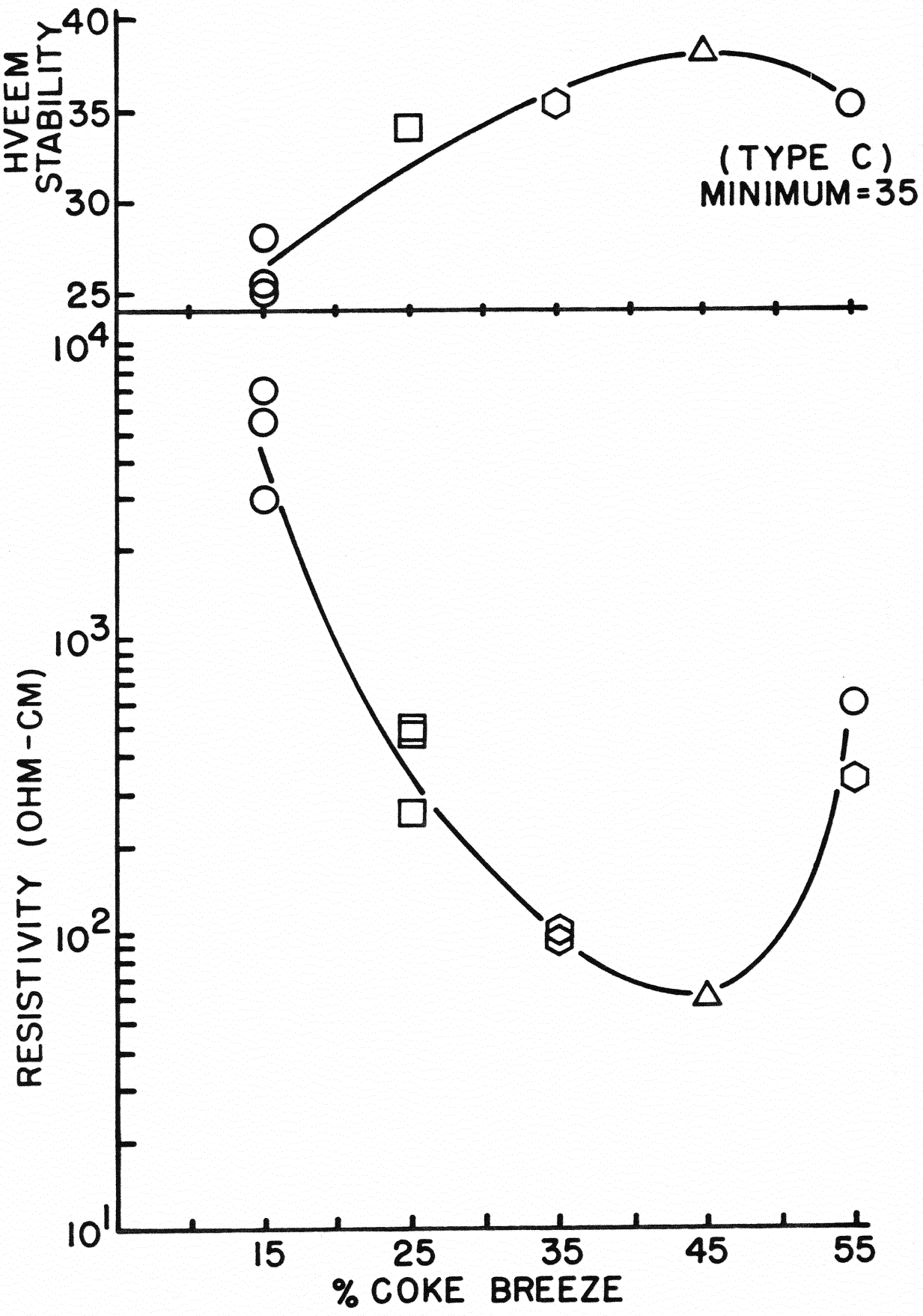
11 % ASPHALT
HVEEM STABILITY
40
35
30
25
(TYPE C)
MINIMUM=35
10^4
10^3
10^2
10^1
RESISTIVITY (OHM-CM)
15
25
35
45
55
% COKE BREEZE

FIG. 11

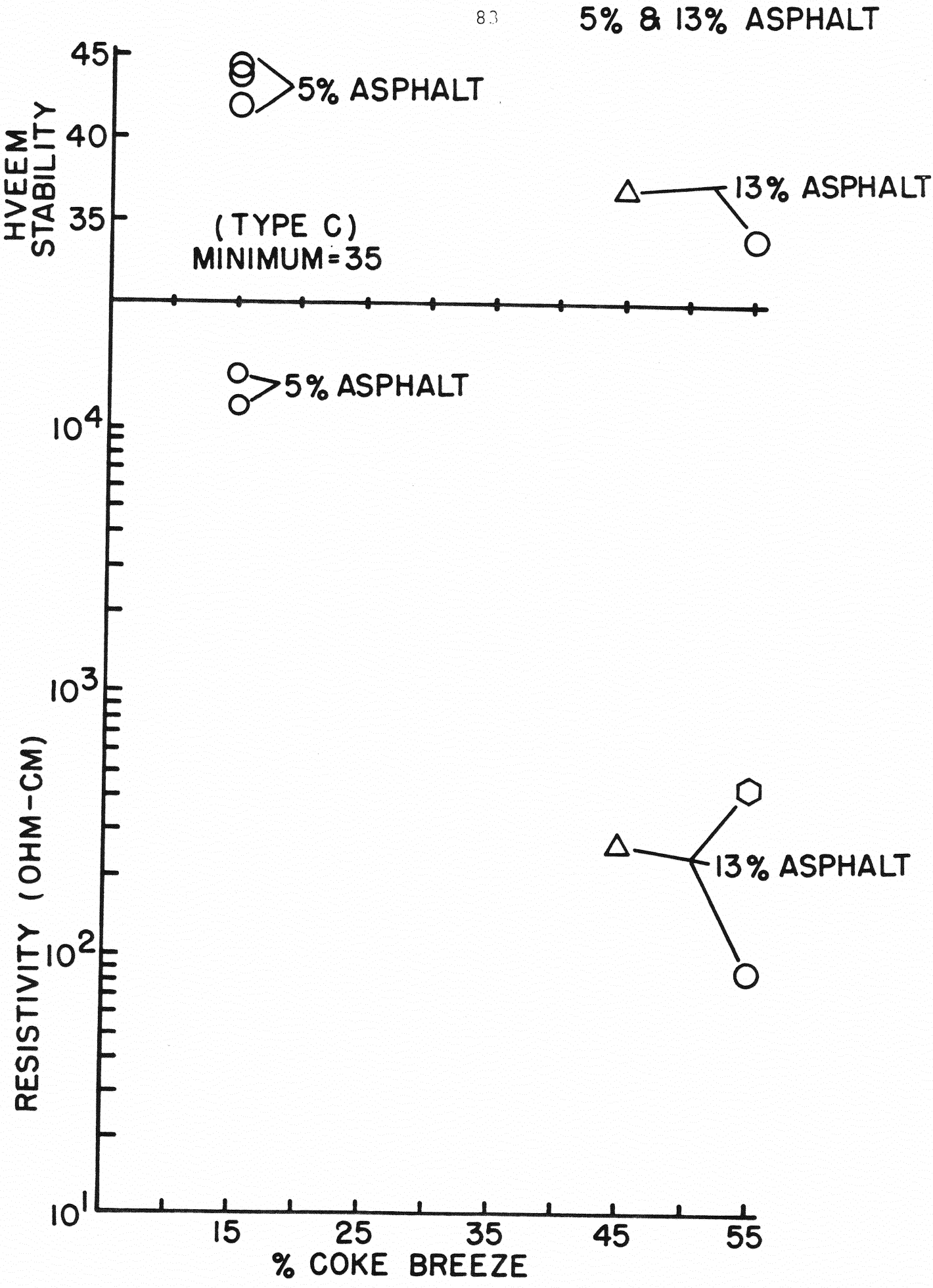
5% & 13% ASPHALT
45
40
35
HVEEM STABILITY
5% ASPHALT
13% ASPHALT
(TYPE C)
MINIMUM=35
5% ASPHALT
10^4
10^3
10^2
10^1
RESISTIVITY (OHM-CM)
13% ASPHALT
15
25
35
45
55
% COKE BREEZE

FIG. 12

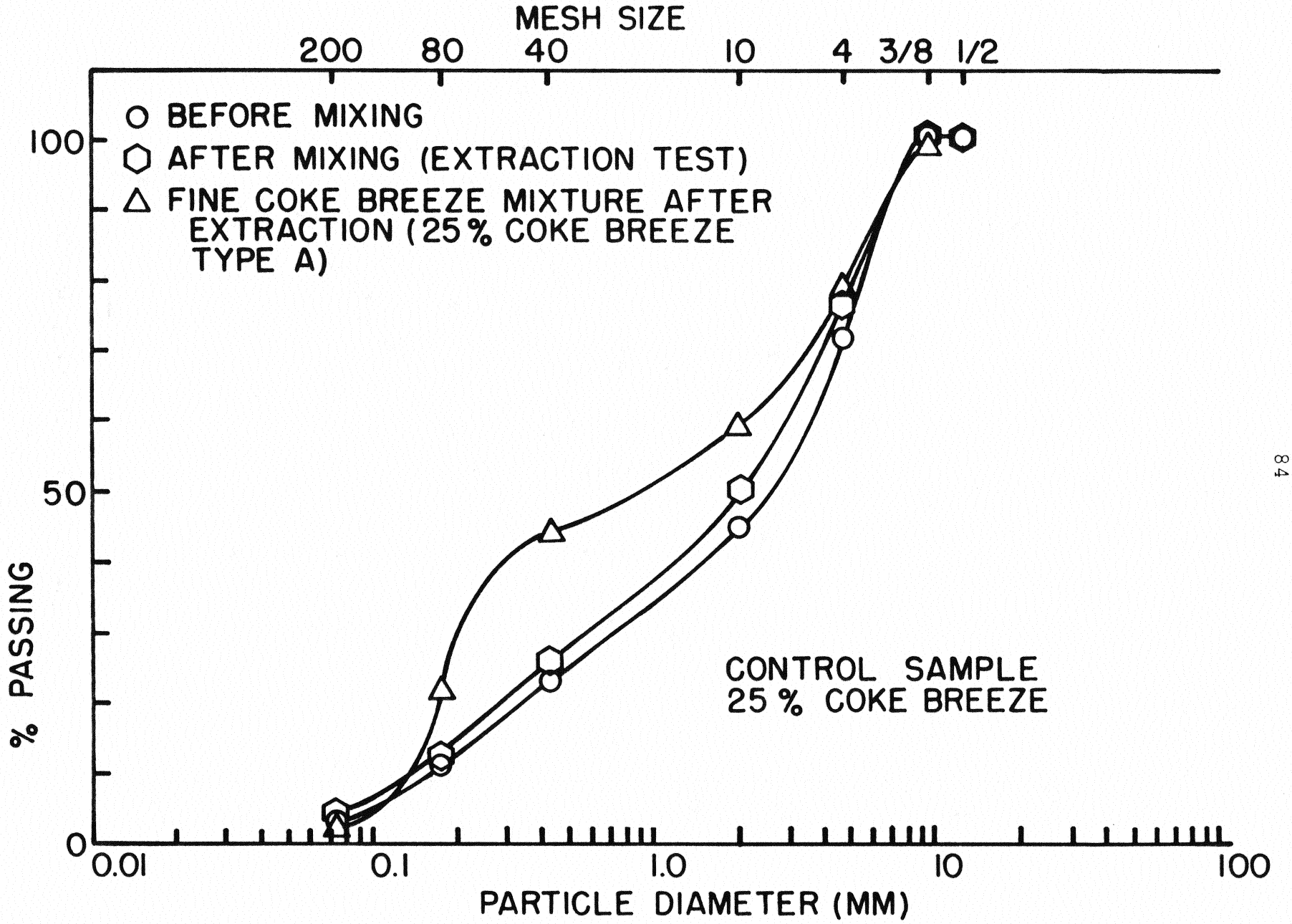
MESH SIZE
200
80
40
10
4
3/8
1/2
BEFORE MIXING
AFTER MIXING (EXTRACTION TEST)
FINE COKE BREEZE MIXTURE AFTER EXTRACTION (25% COKE BREEZE TYPE A)
CONTROL SAMPLE
25% COKE BREEZE
% PASSING
100
50
0
0.01
0.1
1.0
10
100
PARTICLE DIAMETER (MM)

Fig. 13

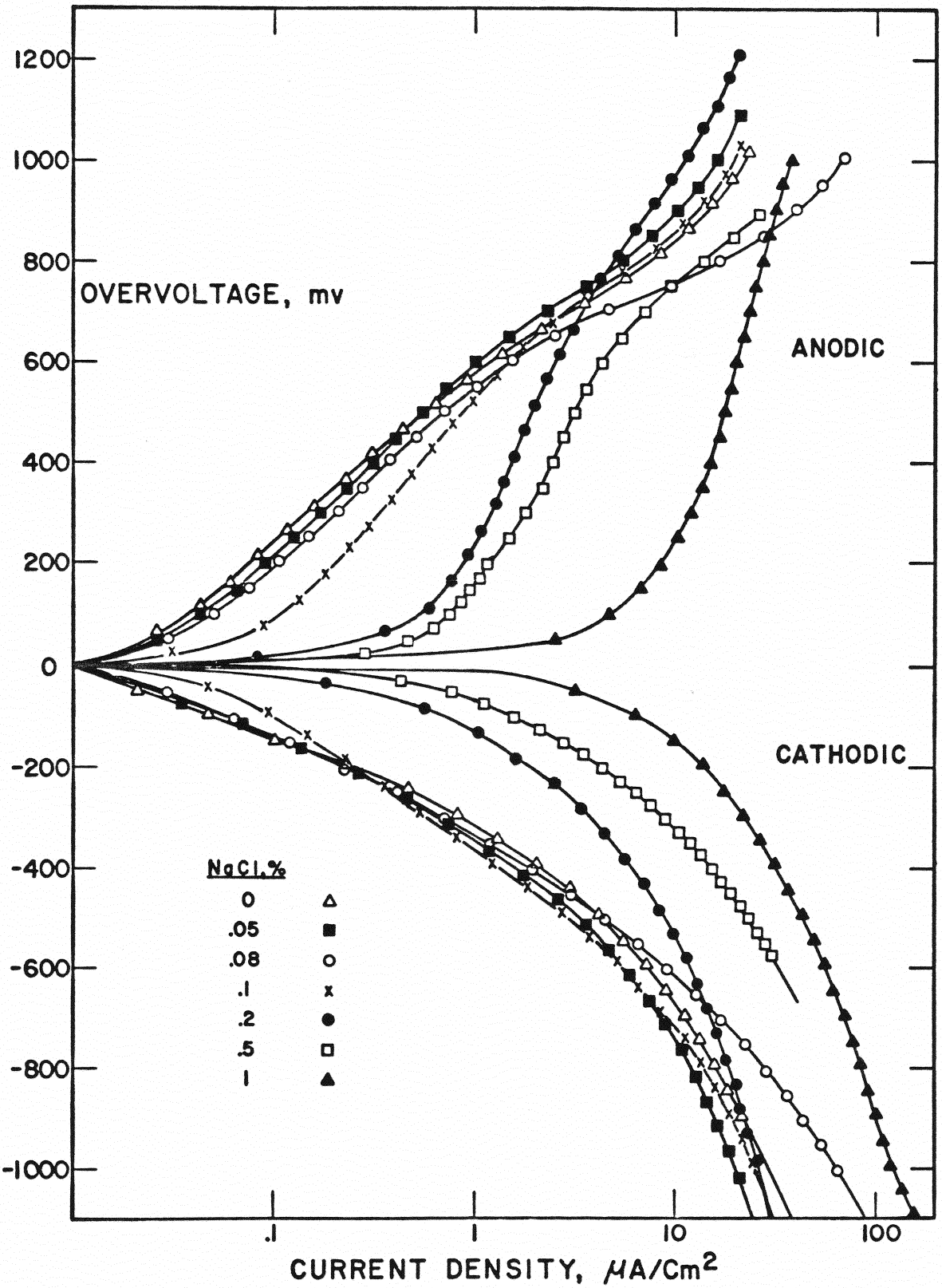
1200
1000
800
600
400
200
0
-200
-400
-600
-800
-1000
OVERVOLTAGE, mv
ANODIC
CATHODIC
NaCl,%
0
.05
.08
.1
.2
.5
1
.1
1
10
100
CURRENT DENSITY, μA/Cm²

FIG. 14

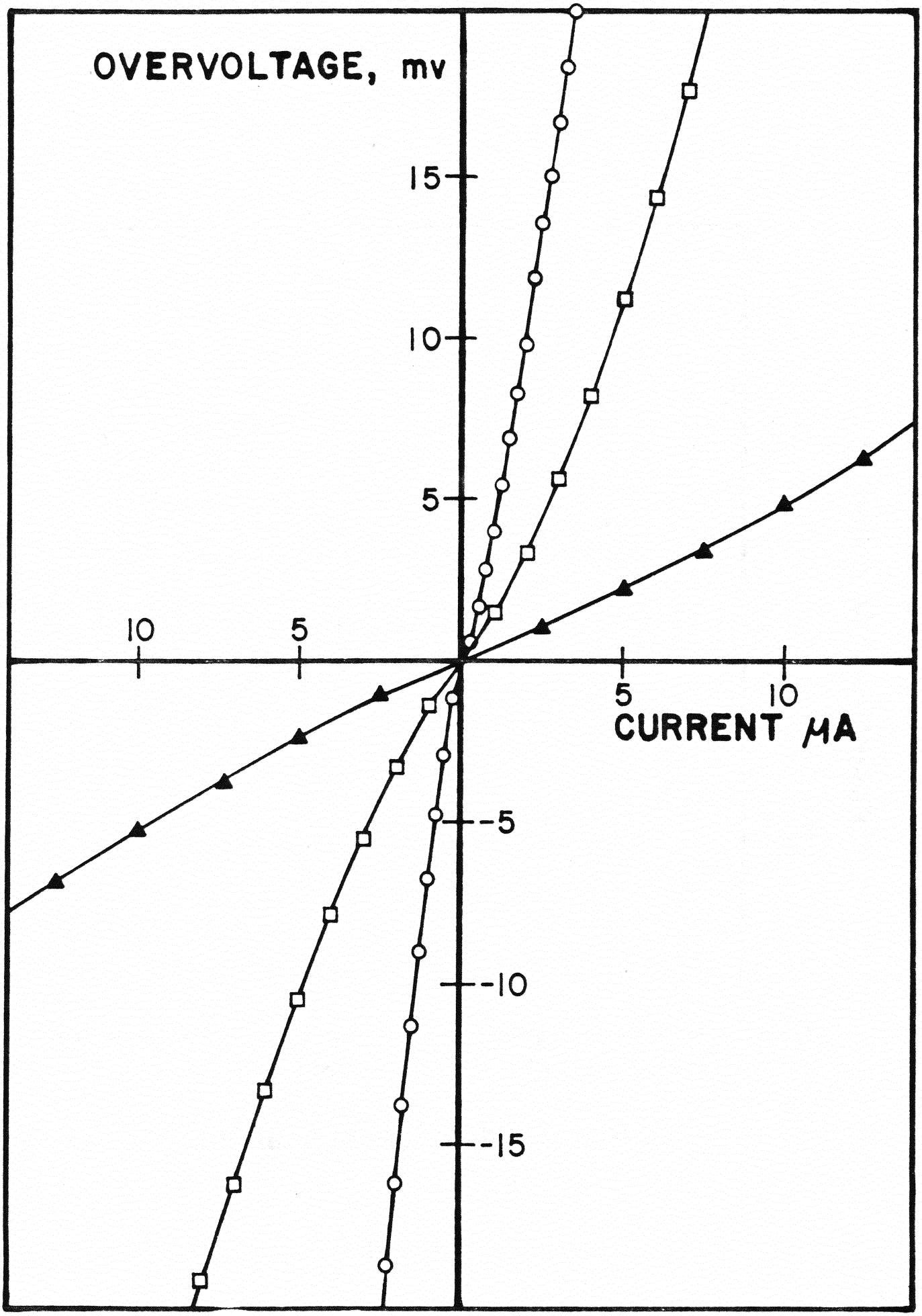

FIG. 15

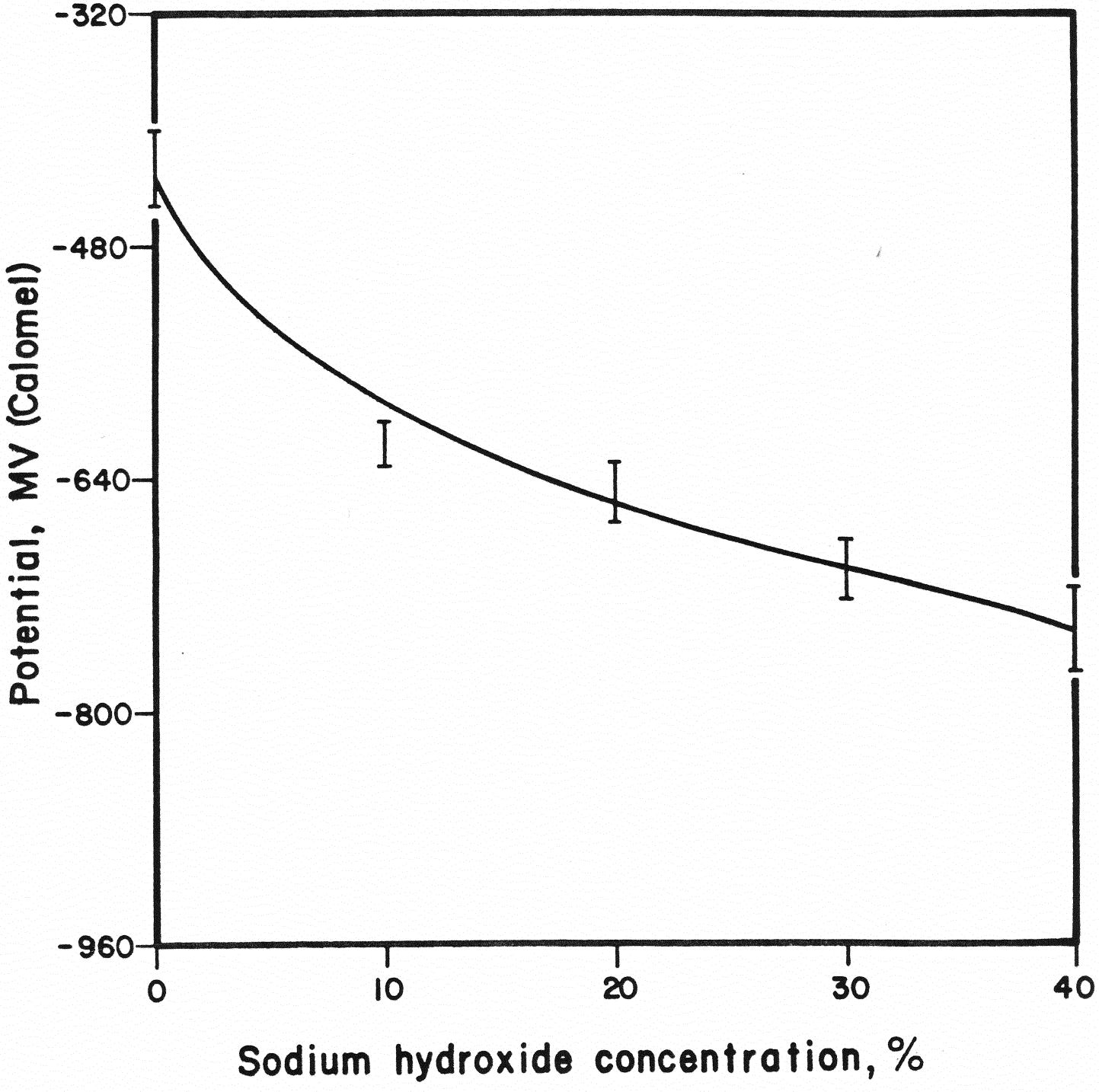
-320
-480
-640
-800
-960
Potential, MV (Calomel)
0
10
20
30
40
Sodium hydroxide concentration, %

FIG. 16

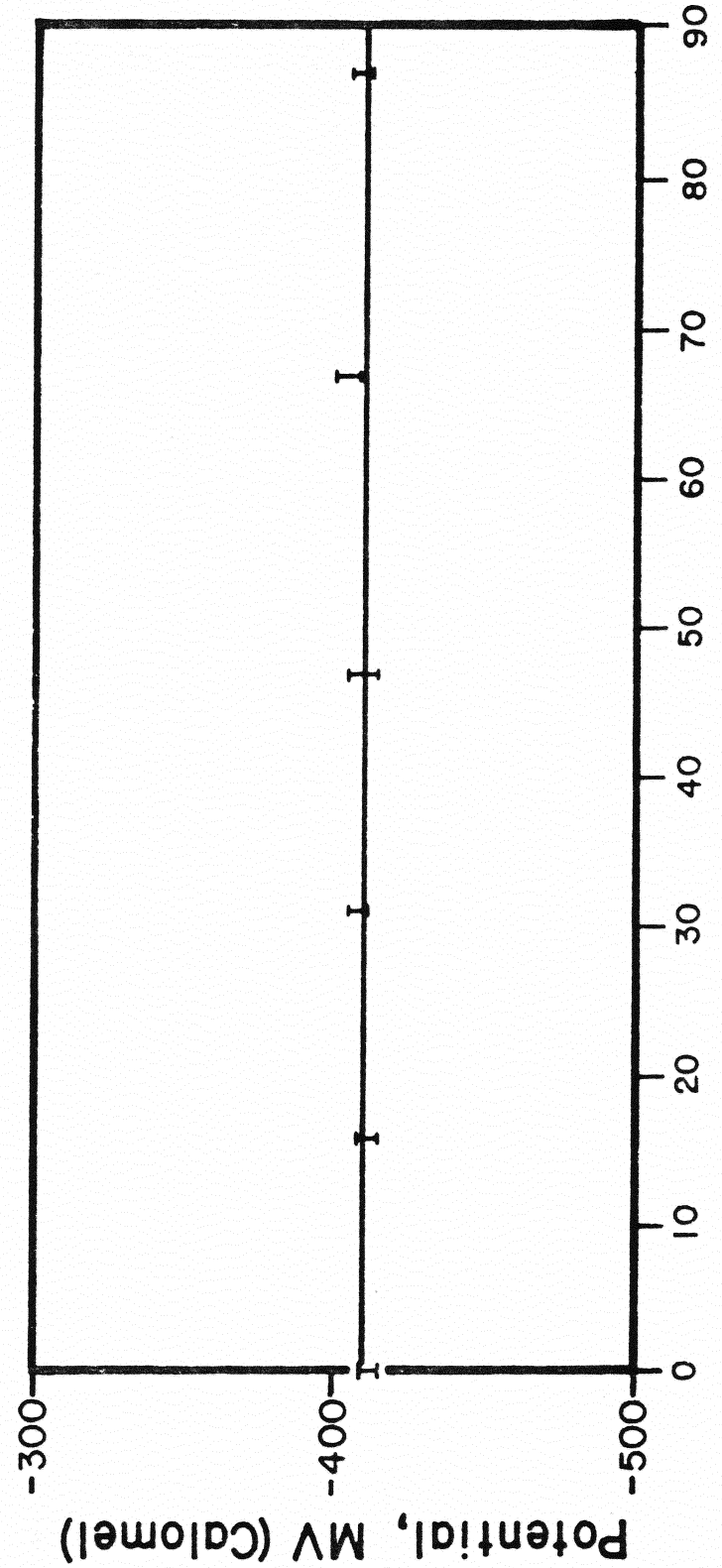
Potential, MV (Calomel)
-300
-400
-500
0
10
20
30
40
50
60
70
80
90
Time (Days)

FIG. 17

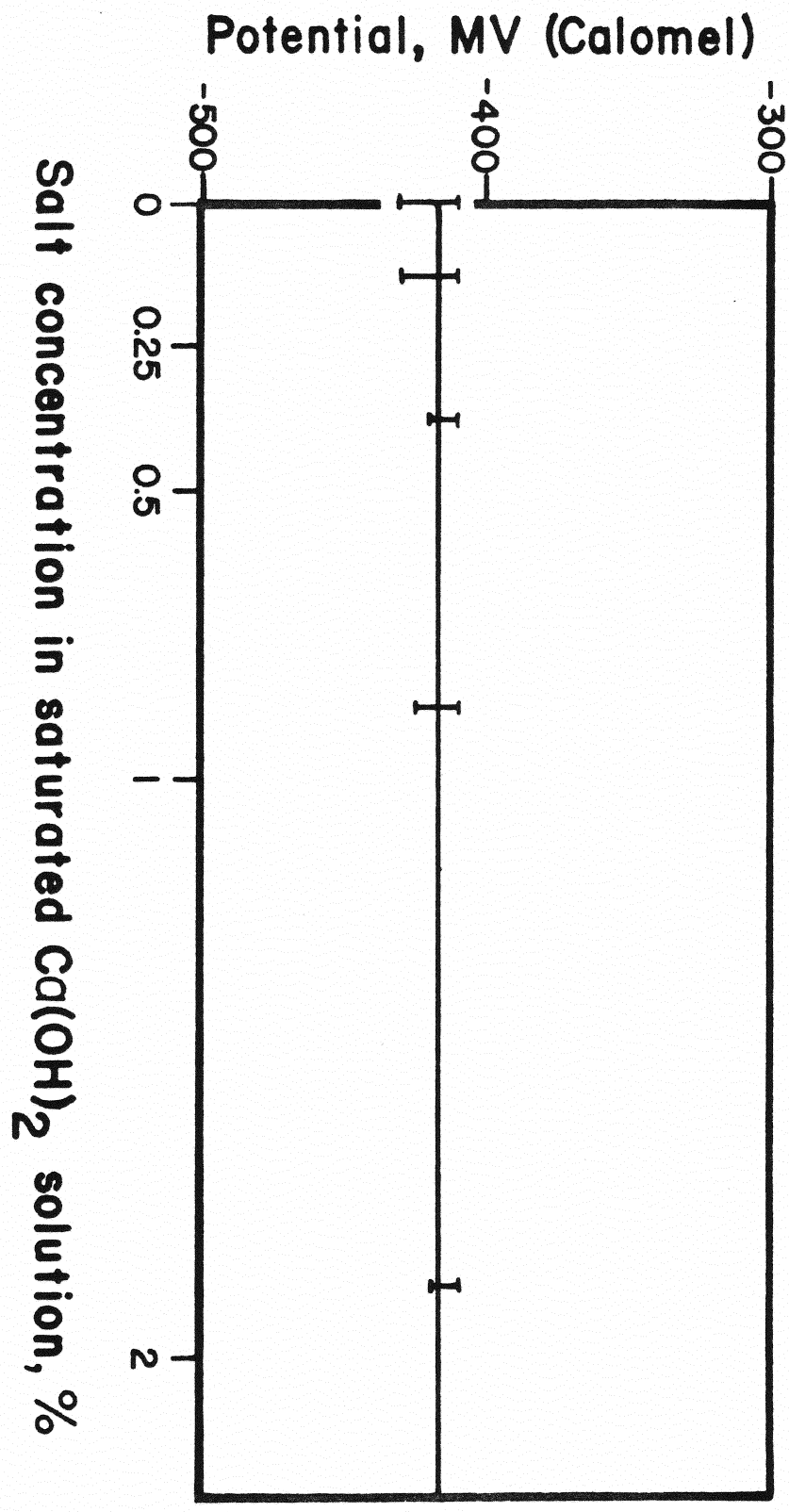
Potential, MV (Calomel)
-500
-400
-300
0
0.25
0.5
1
2
Salt concentration in saturated Ca(OH)2 solution, %

FIG. 18

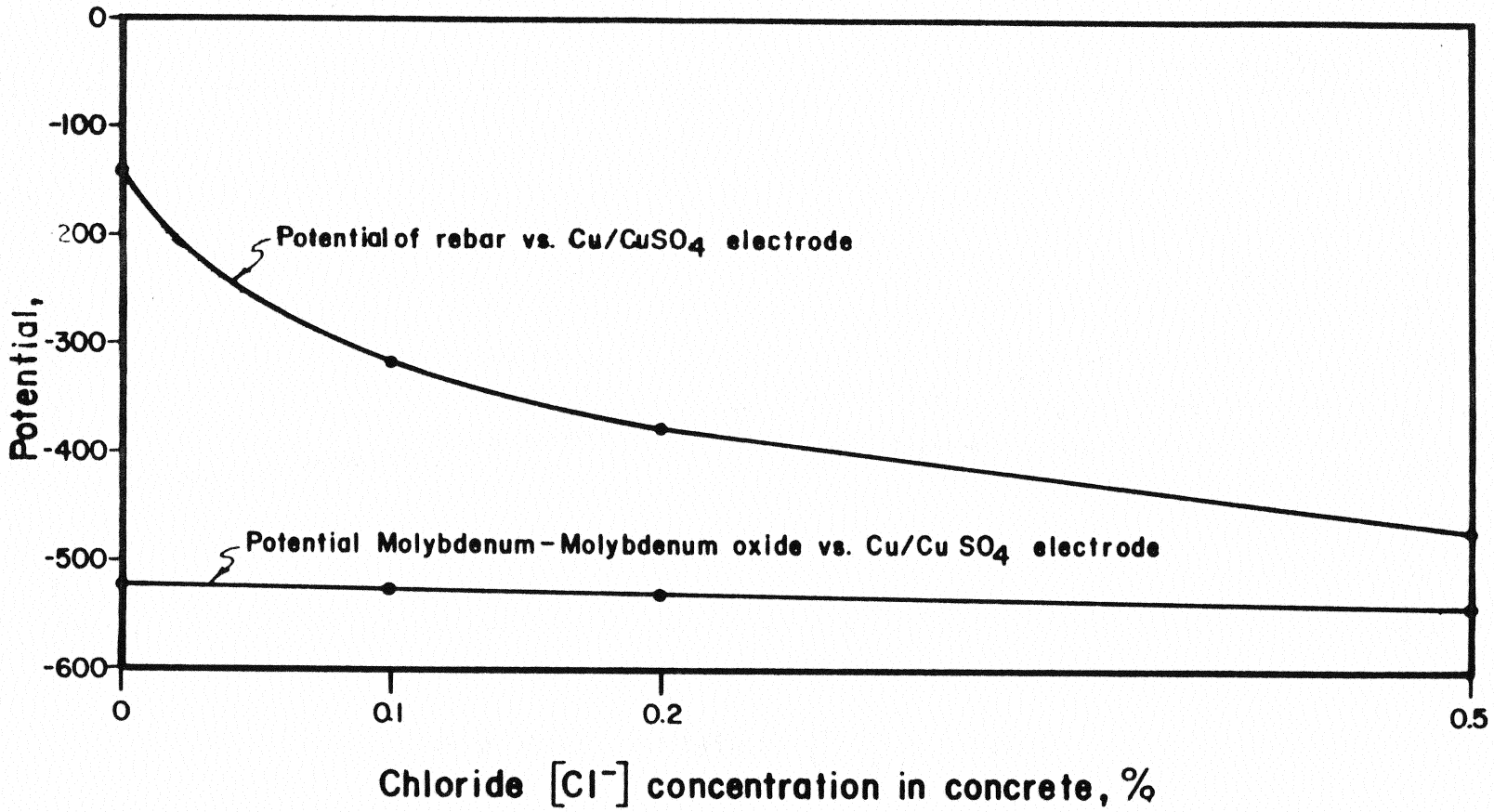
0
-100
-200
-300
-400
-500
-600
Potential,
Potential of rebar vs. Cu/CuSO4 electrode
Potential Molybdenum-Molybdenum oxide vs. Cu/Cu SO4 electrode
0
0.1
0.2
0.5
Chloride [Cl⁻] concentration in concrete, %

FIG. 19

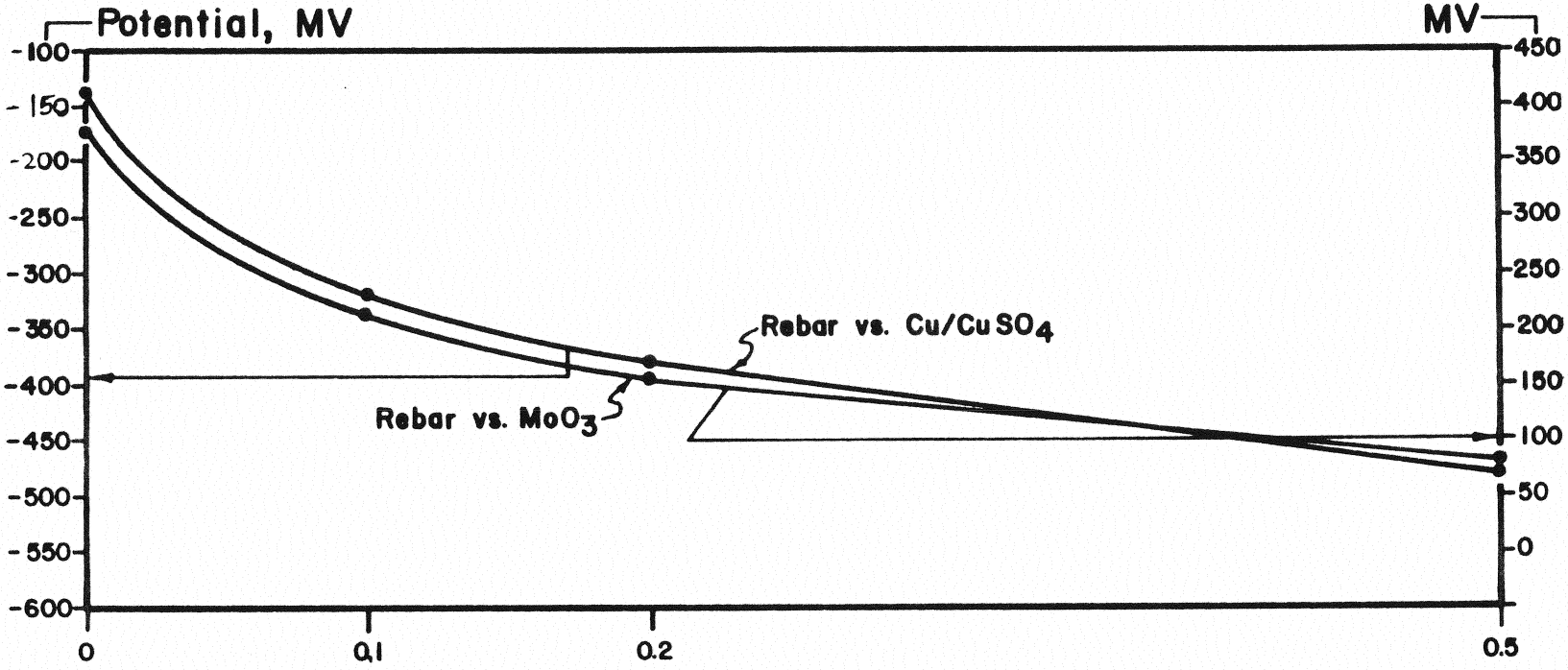
Potential, MV
MV
-100
-150
-200
-250
-300
-350
-400
-450
-500
-550
-600
450
400
350
300
250
200
150
100
50
0
0
0.1
0.2
0.5
Rebar vs. Cu/CuSO4
Rebar vs. MoO3
Chloride [Cl⁻] content in concrete

FIG. 20

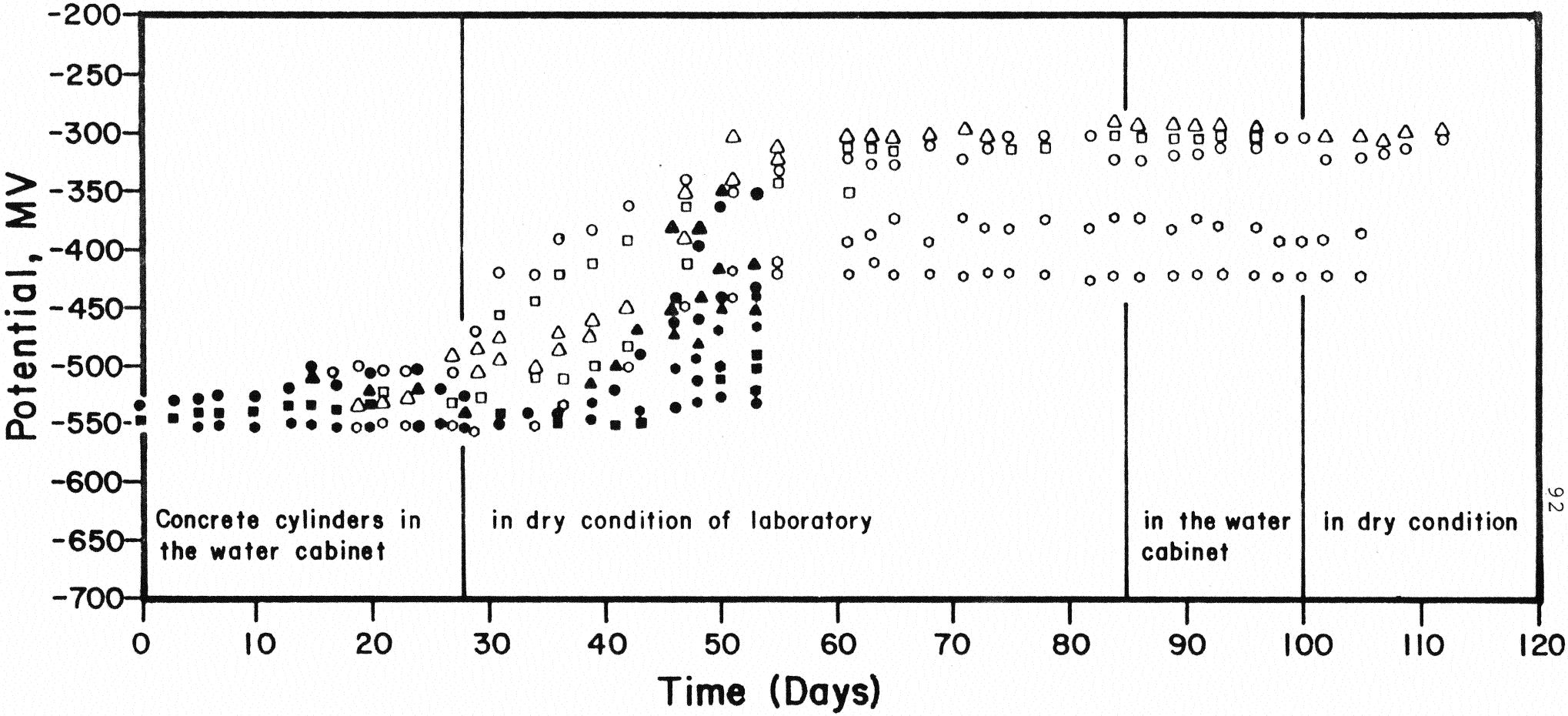

First batch (Silicone seal) Chloride content %	Second batch (Epoxy seal) Chloride content %
0-o	0-●
0.1-△	0.1-▲
0.2-□	0.2-■
0.5-o	0.5-●

FIG. 21

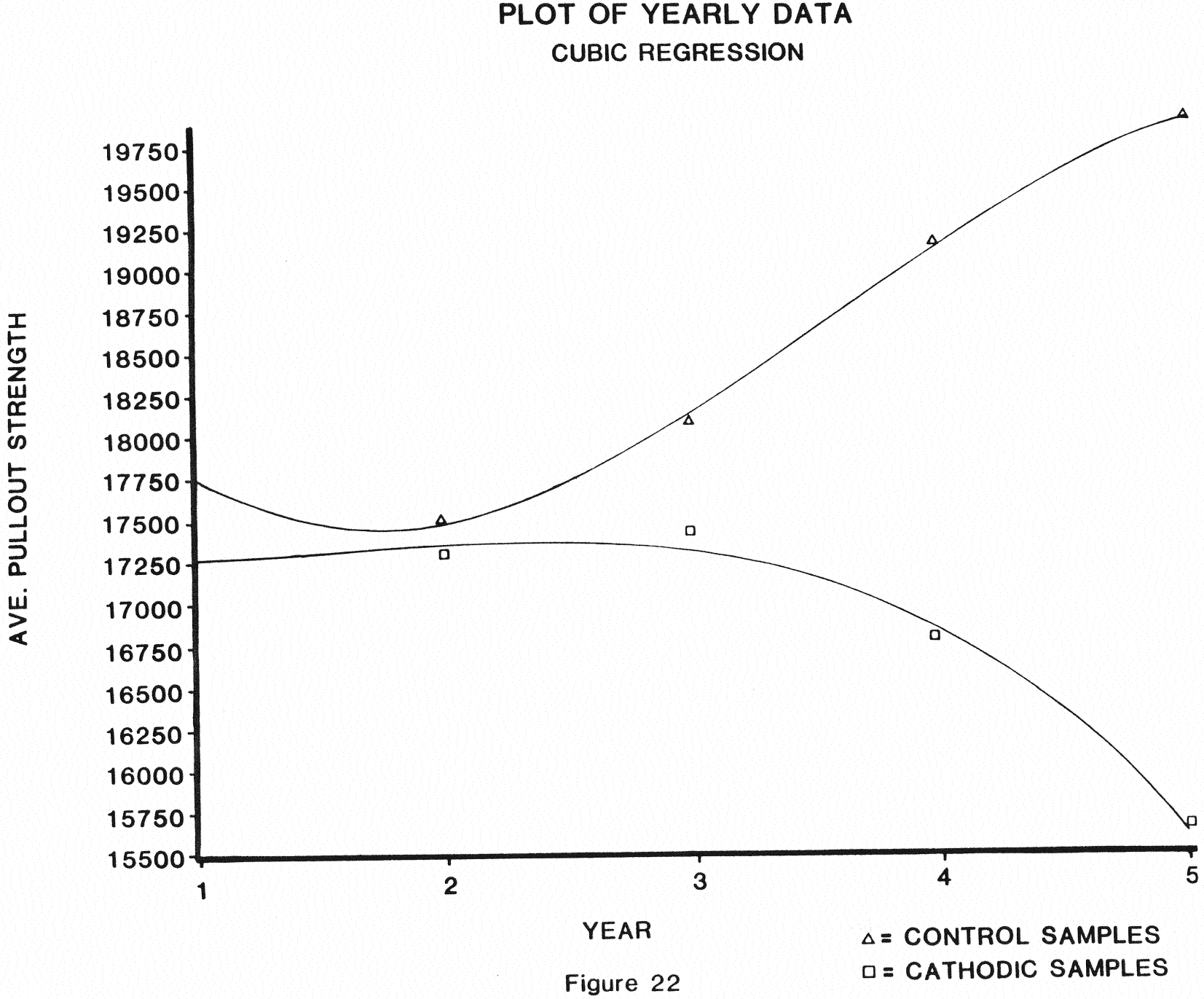
PLOT OF YEARLY DATA
CUBIC REGRESSION
AVE. PULLOUT STRENGTH
19750
19500
19250
19000
18750
18500
18250
18000
17750
17500
17250
17000
16750
16500
16250
16000
15750
15500
1
2
3
4
5
YEAR
△ = CONTROL SAMPLES
□ = CATHODIC SAMPLES

Figure 22

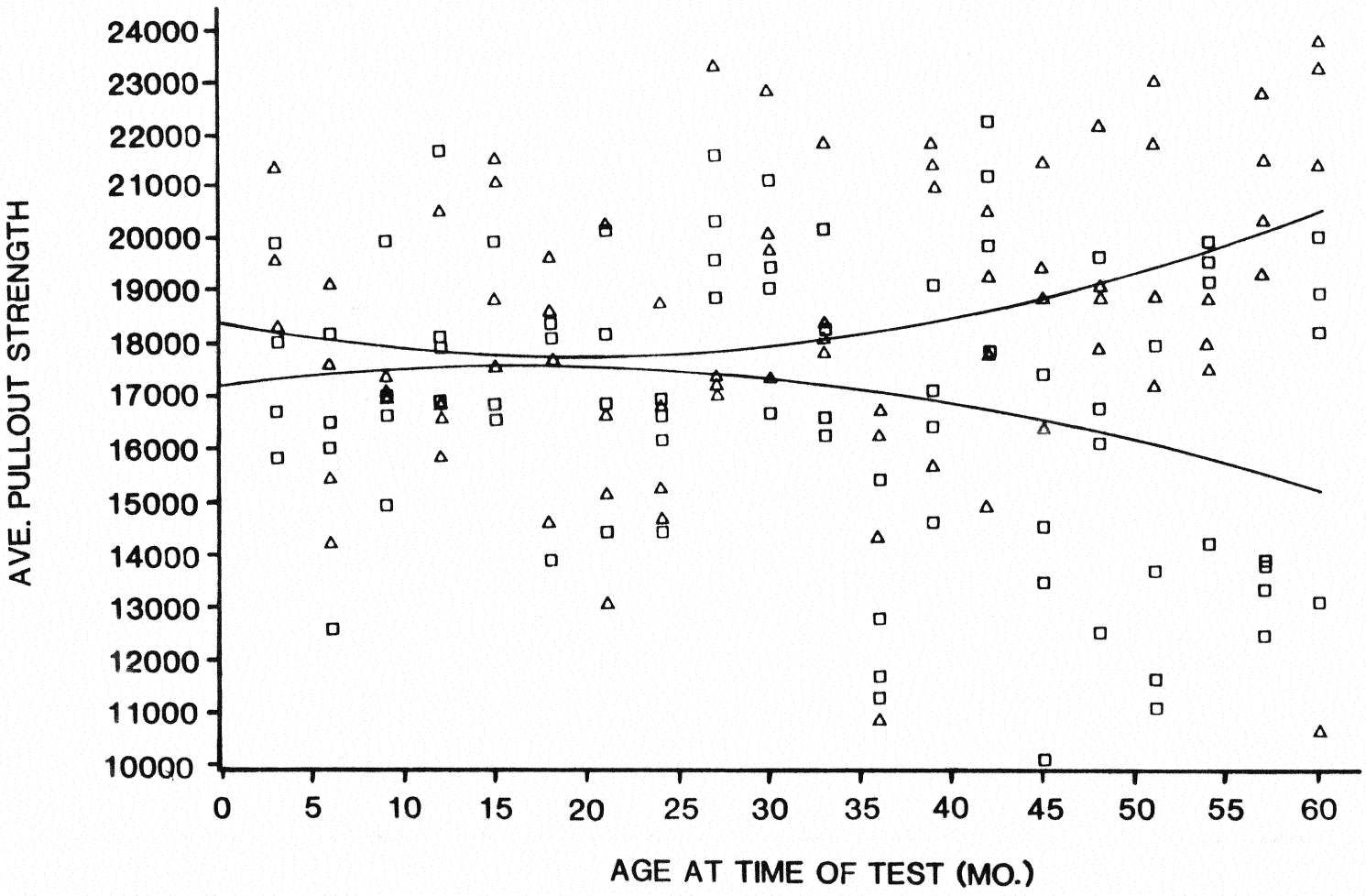
PLOT OF MONTHLY DATA
QUADRATIC REGRESSION
AVE. PULLOUT STRENGTH
24000
23000
22000
21000
20000
19000
18000
17000
16000
15000
14000
13000
12000
11000
10000
0
5
10
15
20
25
30
35
40
45
50
55
60
AGE AT TIME OF TEST (MO.)
LEGEND: STATE CONTROL CP
△ = CONTROL SAMPLES
□ = CATHODIC SAMPLES

Figure 22A

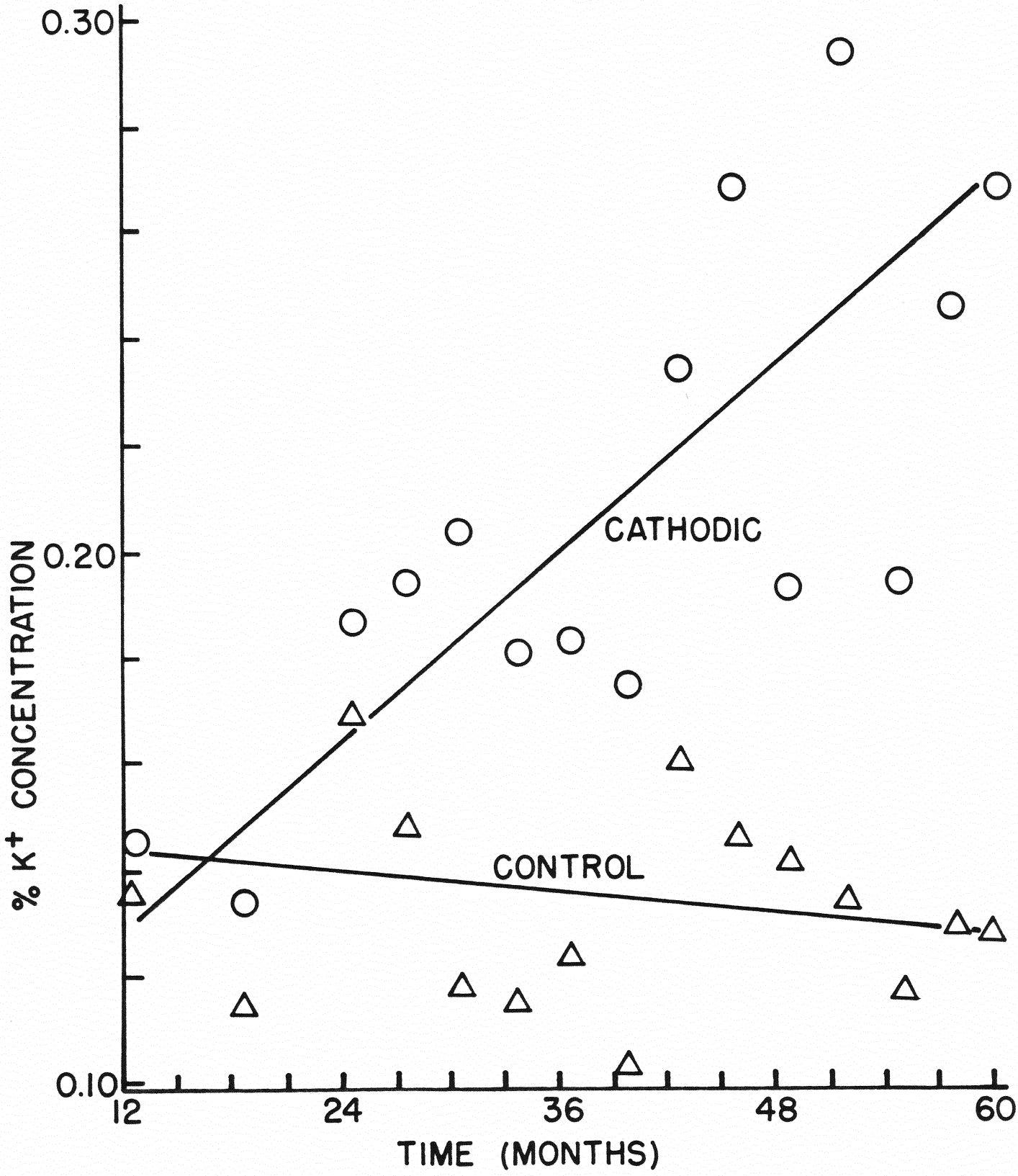

Fig. 23- Concentration of K^+ Near Rebar as a Function of Time

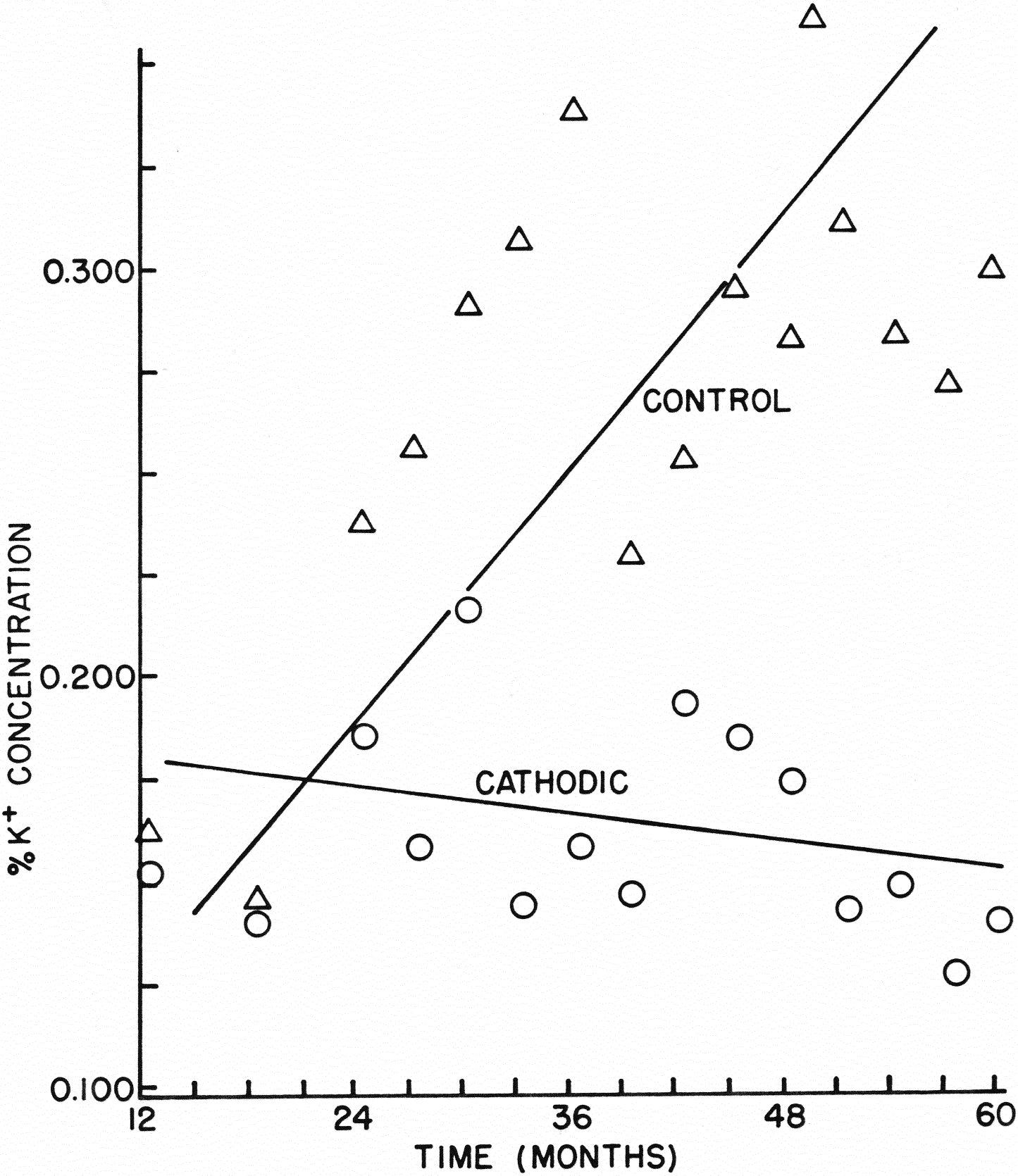

Fig. 24-Concentration of K^+ at the Concrete Surface as a Function of Time

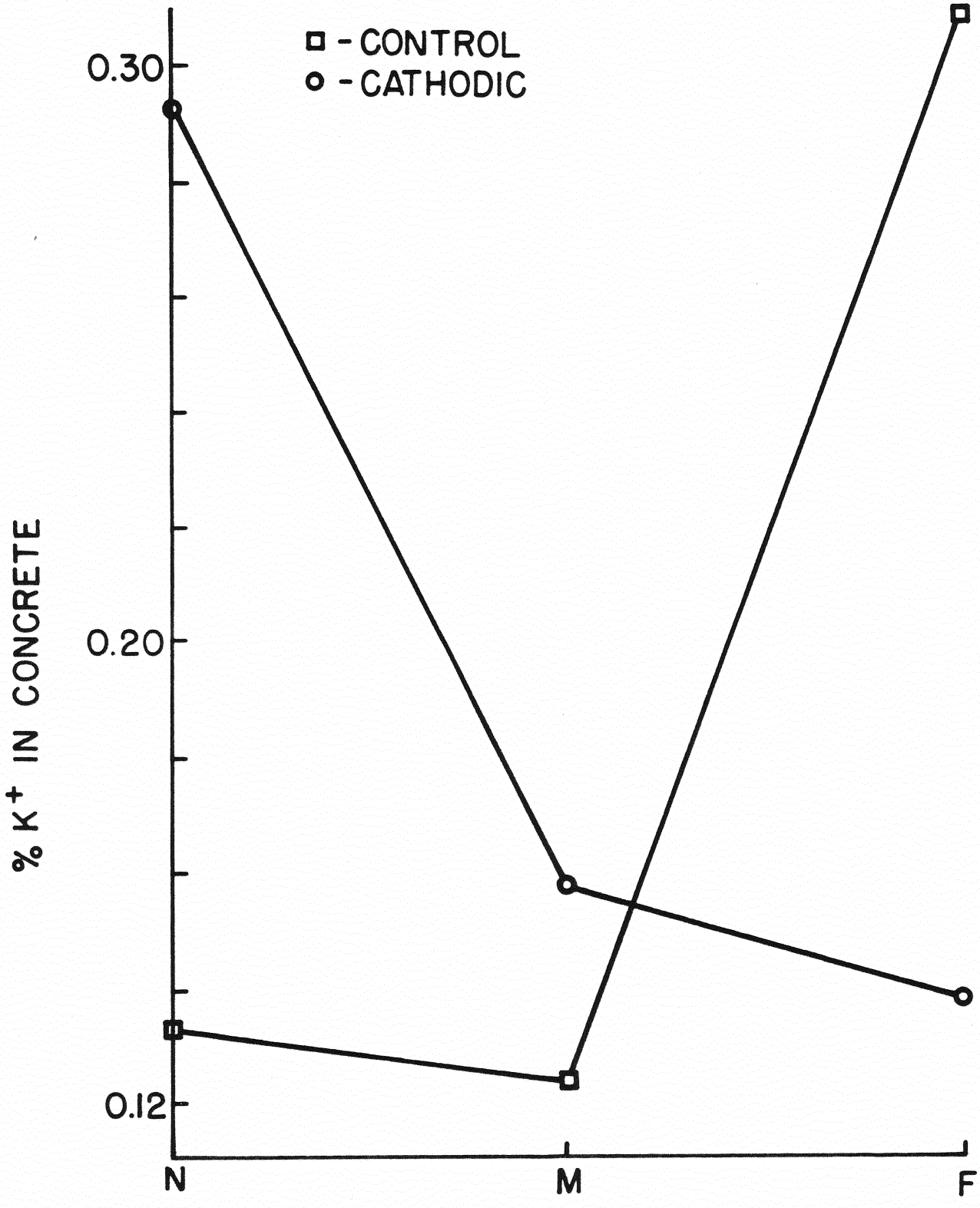

FIG. 25 - K^+ CONCENTRATION VS DISTANCE FROM REBAR

Age, 54 Months

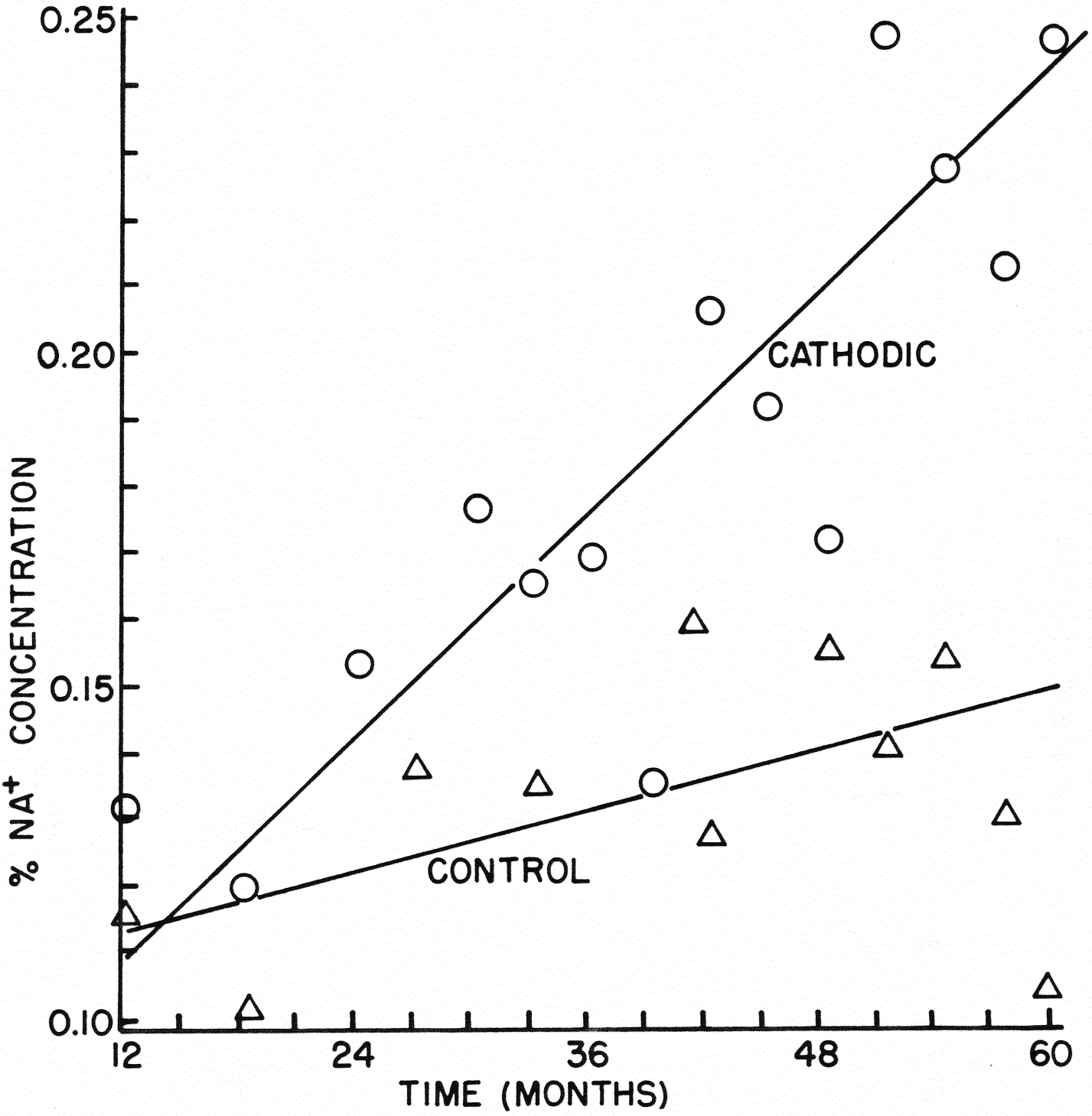

Fig. 26-Concentration of Na^+ Near Rebar as a Function of Time

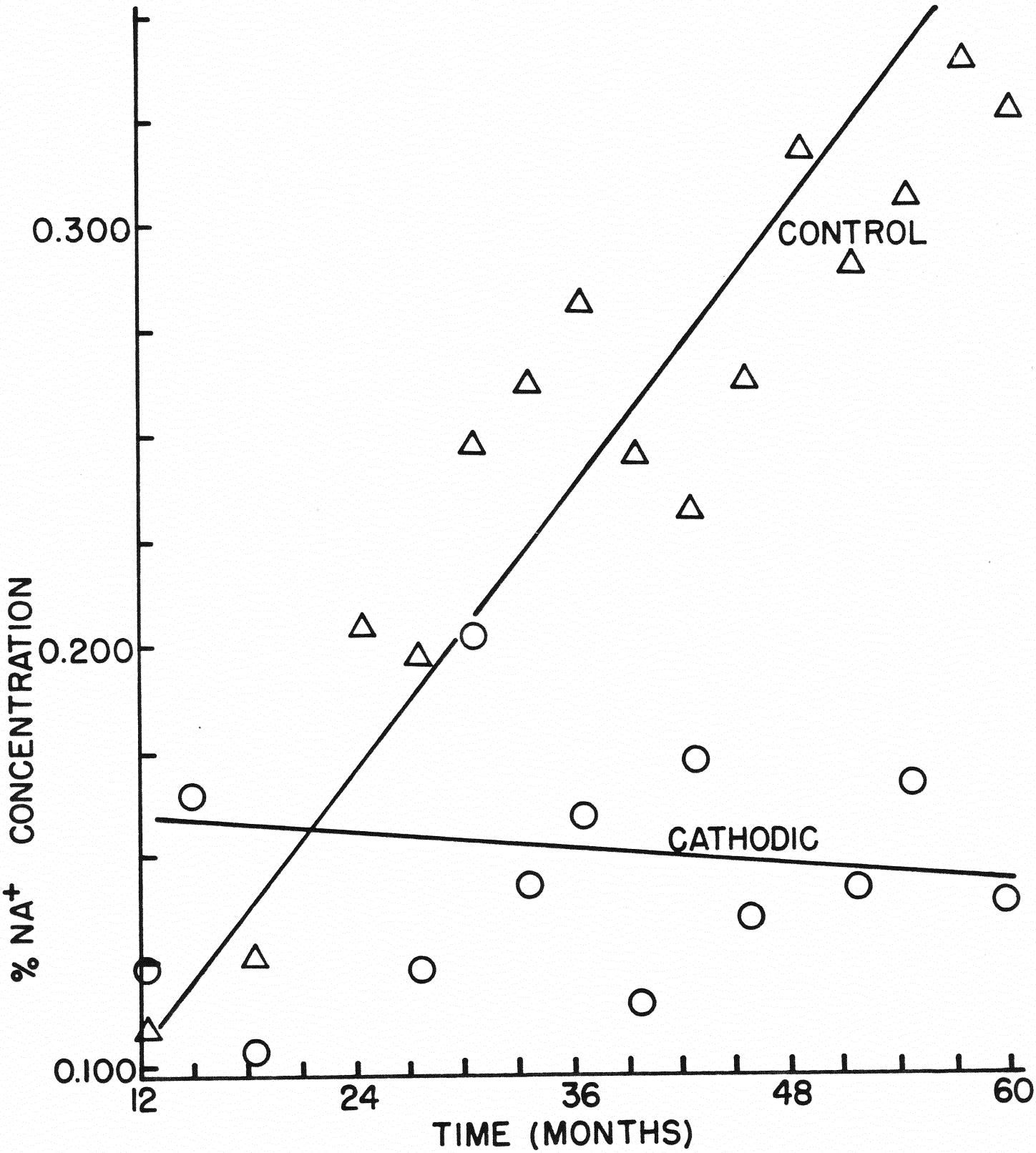

Fig. 27-Concentration of Na^+ at Concrete Surface as a Function of Time

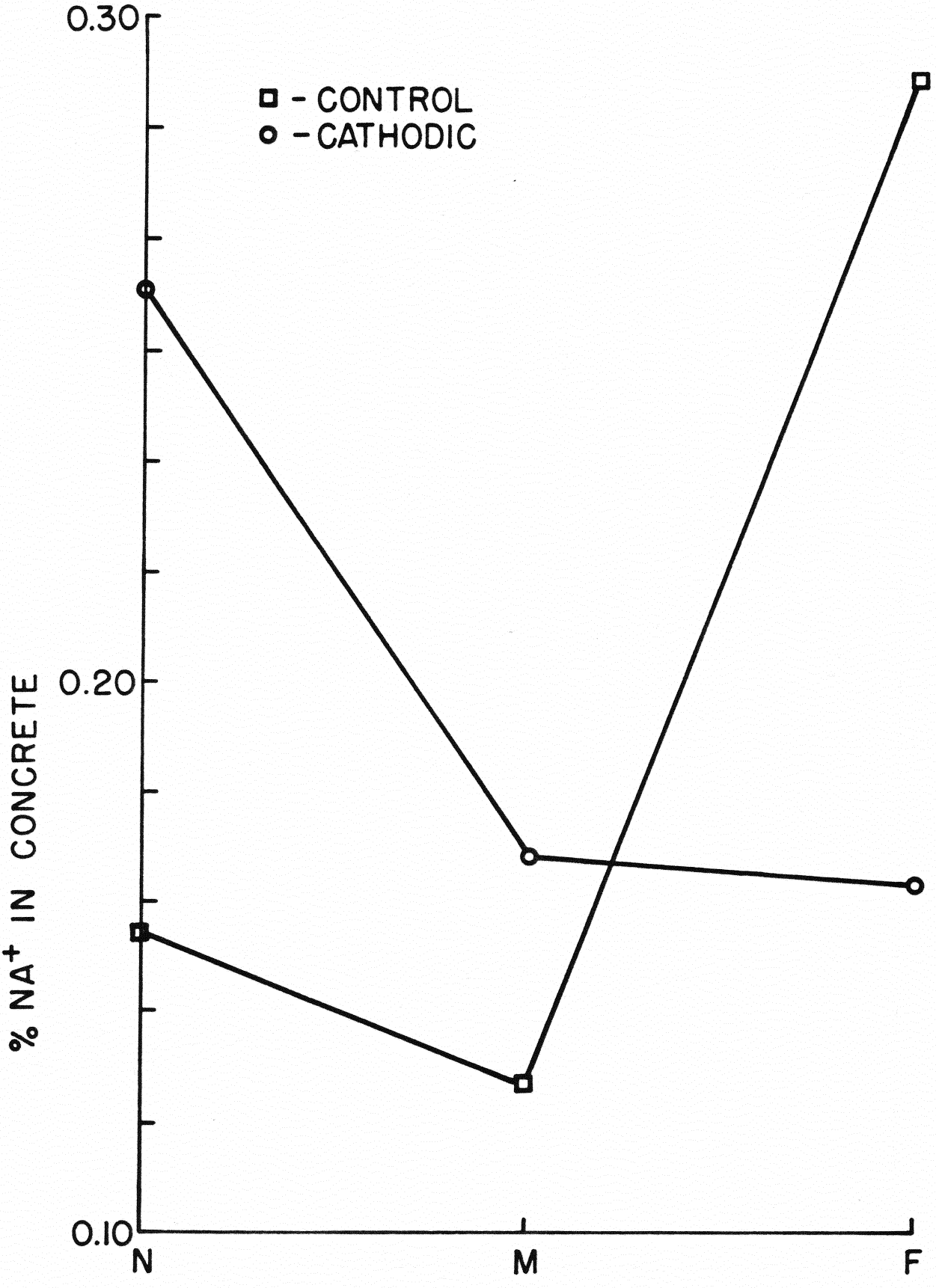

FIG. 28- NA^+ CONCENTRATION VS DISTANCE FROM REBAR

Age, 54 Months

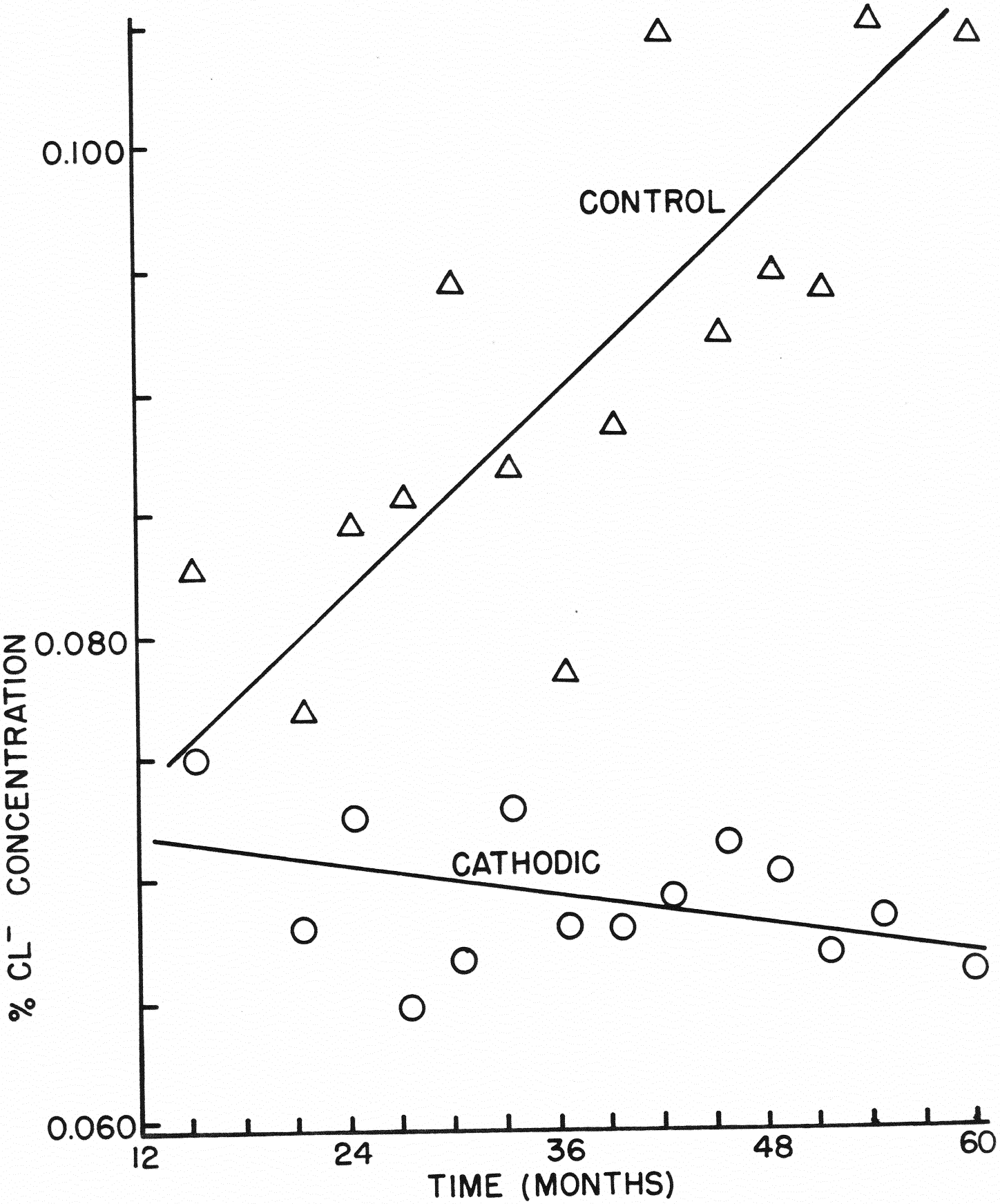

Fig. 29-Concentration of Cl^- Near the Rebar as Function of Time

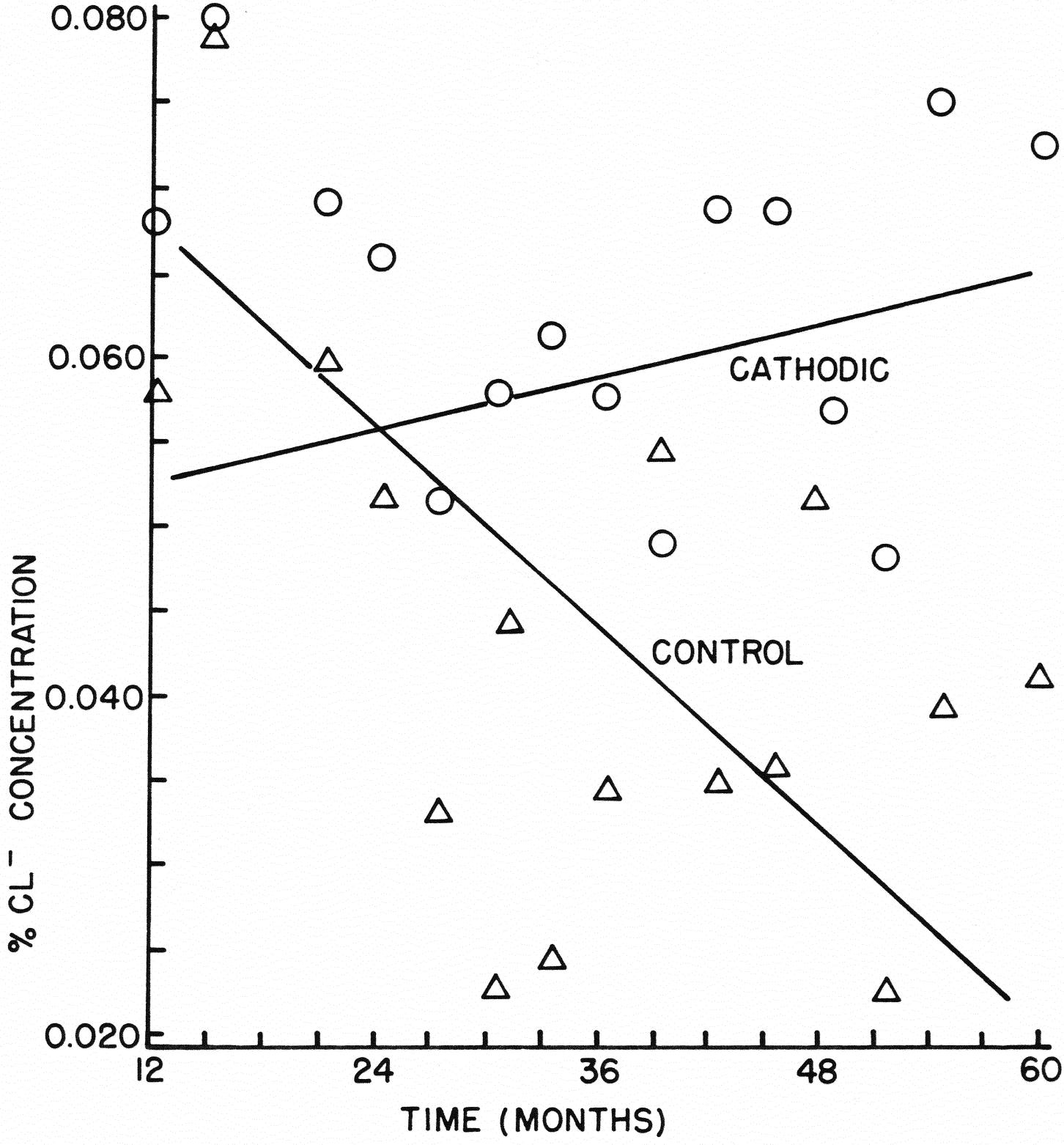

Fig. 30-Concentration of Cl^- at the Concrete Surface as a Function of Time

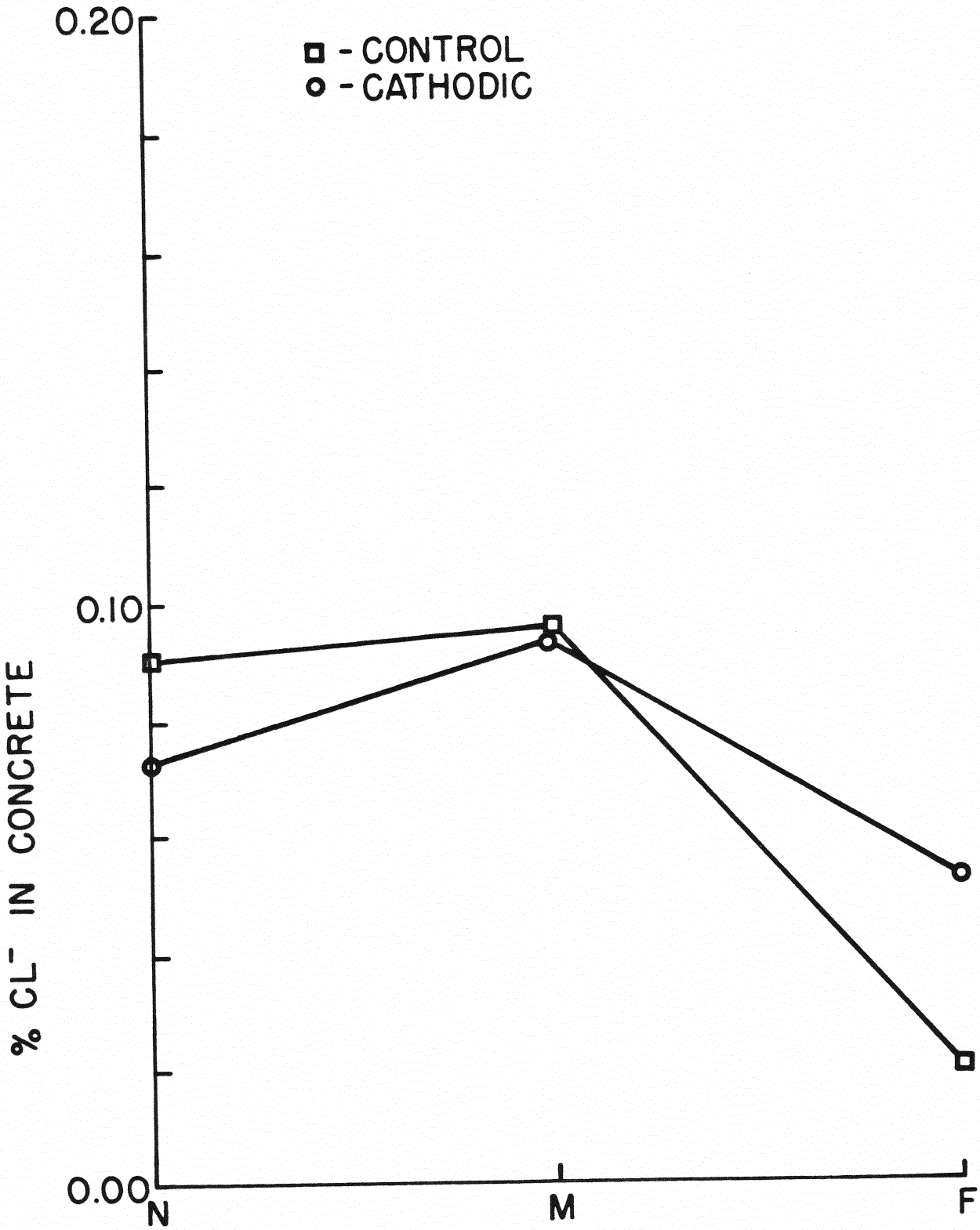

FIG. 31 - CL^- CONCENTRATION VS DISTANCE FROM REBAR

Age, 54 Months